

# Demonstration of Negative Dispersion Fibers for DWDM Metropolitan Area Networks

I. Tomkos, D. Chowdhury, J. Conradi, D. Culverhouse, K. Ennser, C. Giroux, B. Hallock, T. Kennedy, A. Kruse, S. Kumar, N. Lascar, I. Roudas, M. Sharma, R. S. Vodhanel, and C.-C. Wang

**Abstract**—In this paper, we present a detailed experimental and theoretical study, showing that a novel nonzero dispersion-shifted fiber with negative dispersion enhances the capabilities of metropolitan area optical systems, while at the same time, reducing the system cost by eliminating the need of dispersion compensation. The performance of this dispersion-optimized fiber was studied using different types of optical transmitters for both 1310- and 1550-nm wavelength windows and for both 2.5- and 10-Gb/s bit rates. It is shown that this new fiber extends the nonregenerated distance up to 300 km when directly modulated distributed feedback (DFB) laser transmitters at 2.5 Gb/s are used. The negative dispersion characteristics of the fiber also enhance the transmission performance in metropolitan area networks with transmitters that use electroabsorption (EA) modulator integrated distributed feedback (DFB) lasers, which are biased for positive chirp. In the case of 10 Gb/s, externally modulated signals (using either EA-DFBs or external modulated lasers using Mach-Zehnder modulators), we predict that the maximum reach that can be accomplished without dispersion compensation is more than 200 km for both 100- and 200-GHz channel spacing. To our knowledge, this is the first demonstration of the capabilities of a nonzero dispersion-shifted fiber with negative dispersion for metropolitan applications.

## I. INTRODUCTION

**D**ENSE wavelength-division-multiplexing (DWDM) technologies are being deployed internationally, since it is recognized that they can satisfy the traffic demands for high-capacity networking. The last two years have marked the introduction of DWDM also in metropolitan area networks [1], [2]. The unique characteristics of the metro environment, such as high sensitivity to price, as well as the immaturity of the technology have been its main obstacles to widespread deployment to date. Several research projects such as Optical Networks Technology Consortium (ONTC) [3], Multiwavelength Optical NETWORKing (MONET) [4] and All-Optical Network (AON) [5], had previously focused on applying DWDM in the long-haul and metro environment. The increasing demand for more bandwidth in the access network, created by the need for enhanced services mainly through the Internet, and the availability of optical components at a competitive price are now beginning to shift the network

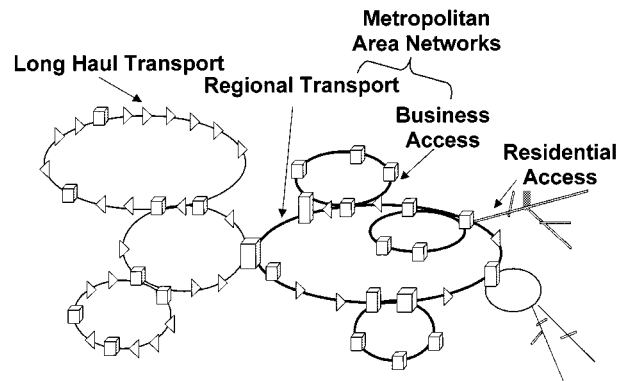


Fig. 1. The structure of DWDM optical networks.

prototypes from the research labs to the field, signaling the rise of DWDM in the metro environment [1], [2]. Fig. 1 shows a simplified picture of the layout of optical networks. Metro optical networks, interfacing both the long-haul and the residential access networks, may encompass regional through business-access networks. Typically, their size can be up to 300 km, and the bit rate per wavelength can be either 2.5 or 10 Gb/s. Metro systems differ from long-haul DWDM systems in that they are far more sensitive to equipment costs, requiring the use of low-cost optical components.

In metro area networks, the dispersion-induced waveform distortion is the major impairment that the designer of the system has to consider. Depending on the choice of the optical transmitter and consequently its frequency-chirp characteristics, the dispersion-induced waveform distortion can be deleterious for the signal transmission, even at very short distances. Dispersion compensation is used in point to point long-haul systems to reduce dispersion-induced penalties. However, in optical networks the placement of the dispersion compensating modules (DCM) becomes an issue because (a) different optical channels in a fiber originate from different nodes, and hence, see different amounts of accumulated dispersion, (b) the loss added by the dispersion compensating modules increases the effective noise figure of the system and limits the size of the network in noise-limited systems, and (c) dispersion compensation adds cost. Therefore, an optical fiber with dispersion-optimized design for Metro area applications that will eliminate the need for dispersion compensation should ease the engineering of the network.

The choice of the optical transmitter and its associated characteristics will determine the maximum distance that the signal can be transmitted. Depending on the per wavelength bit rate, different types of optical transmitters are considered, including

Manuscript received July 17, 2000; revised May 17, 2001.

I. Tomkos, K. Ennser, B. Hallock, T. Kennedy, A. Kruse, N. Lascar, I. Roudas, M. Sharma, R. S. Vodhanel, and C.-C. Wang are with the Corning Inc., Science and Technology, Photonics Research and Test Center, PRTC, Corning Inc., Somerset, NJ 08873 USA (e-mail: tomkosi@corning.com).

D. Chowdhury, J. Conradi, D. Culverhouse, C. Giroux, and S. Kumar are with the Science and Technology Division Corning Incorporated, Corning, NY 14831 USA.

Publisher Item Identifier S 1077-260X(01)08943-2.

directly modulated distributed feedback lasers (DMLs), electroabsorption modulated distributed feedback lasers (EA-DFBs) or externally modulated lasers using Mach–Zehnder LiNbO<sub>3</sub> modulators (MZ). In all cases, semiconductor distributed feedback laser sources are assumed.

Low-cost directly modulated lasers (DML) recently attracted much attention for use as transmitters in 2.5-Gb/s metro area applications. However, DMLs have some major drawbacks. The output power waveform is not an exact replica of the modulation current and the instantaneous optical frequency varies with time depending on the changes of the optical power (an effect also known as frequency chirp) [6], [7]. The interaction of the positive chirp with the positive dispersion of conventional standard single-mode fibers (like Corning SMF-28 fiber or any other fiber with similar dispersion characteristics) deteriorates the optical signal and sets a limit in the maximum achievable transmission distance [7]–[9]. The dispersion-induced waveform distortion is the major impairment limiting the size of the metropolitan area systems using SMF-28 fiber. Typically, DMLs are rated for 100-km transmission distances over SMF-28 fiber with less than 2-dB dispersion-induced penalty. Therefore, for such systems, there is a growing interest to use a fiber whose dispersion is optimized for increased transmission distance with DMLs. Negative dispersion fibers can be used to take advantage of the positive chirp characteristics of DMLs to enhance transmission distances [10].

Electroabsorption modulator integrated distributed feedback lasers have recently attracted much attention as cost-effective transmitters for 10-Gb/s (OC-192) applications. The average  $\alpha$ -parameter of an electroabsorption-modulated laser is tunable, depending on the value of the reverse bias voltage applied to the modulator section of the EA-DFB [11], [12]. Change of the reverse bias affects, also the output power [11], [12]. In general, an increase of the reverse bias voltage of the absorption section results in increased absorption, and consequently decreased output optical power, while concurrently the  $\alpha$ -parameter decreases and can even become negative. Since the  $\alpha$ -parameter is tunable, optimum operating-conditions in terms of the chirp/dispersion interactions can be set for fibers having different amounts and signs of dispersion. For example for optimum transmission performance over fibers with positive dispersion, the  $\alpha$ -parameter should be set to have a negative value. Although this is possible for a large reverse bias voltage, the absorption is very large and the output optical power is greatly reduced. Conversely, for negative dispersion fibers, the bias voltage of the EA-DFB can be set for positive chirp to achieve increased transmission distances relative to SMF-28 fiber. This setting provides the added benefit of increased output power, since the absorption at the EA section is reduced when biased for positive chirp [11], [12].

The choice of external modulation using Mach–Zehnder (MZ) modulators is far more expensive, but it can be also considered for 10-Gb/s metro area applications. The characteristics of the chirp parameter of MZ modulators is different from that of electroabsorption integrated DFB lasers [12], and therefore, is studied separately. The commercially available modulators can produce chirp-free signals or can be used for prechirping. In the latter case, the chirp-parameter can be either +0.7 or

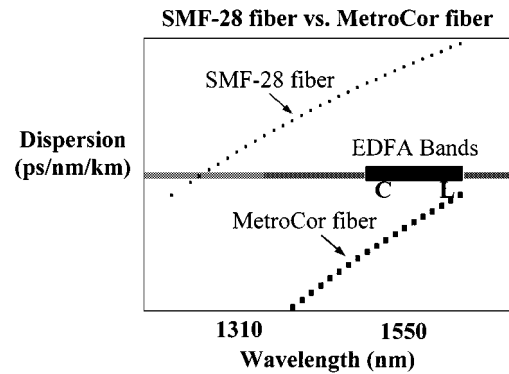


Fig. 2. The dispersion characteristics of MetroCor and SMF-28 fibers.

−0.7. Thus, in the following, we will limit our studies to the specific chirp-parameter values.

Recently, a nonzero dispersion-shifted fiber (NZDSF) with negative dispersion (Corning MetroCor fiber) was introduced to take advantage of the positive chirp characteristics of low-cost transmitters that are likely to be used in metro area networks. This dispersion-optimized optical fiber can eliminate the need for dispersion compensation and will enable the introduction of DWDM technologies in the metro environment. The dispersion characteristics of this novel fiber are shown in Fig. 2. MetroCor fiber has a zero dispersion wavelength  $\lambda_0$  near 1630–1640 nm. As a result, this fiber has an average dispersion of about −3 ps/nm/km in the *L*-band and about −8 ps/nm/km in the *C*-band. The loss, the dispersion slope and the effective area are typical of other conventional NZ-DSF fibers (G.655 compliant fiber).

The idea for the design of a specialty fiber with such dispersion characteristics is based on considerations regarding the interaction of laser frequency chirp with the fiber dispersion. It is known that the chirp greatly affects the pulse propagation by causing the leading and trailing edges of the pulses to have slightly different frequencies and consequently different group velocities. If the  $\alpha$ -parameter (chirp parameter) is positive, as it is always the case for directly modulated lasers, then the frequency components of the leading edge of the pulse will be blue-shifted and the trailing edge red-shifted.<sup>1</sup> In general, if the pulses are transmitted over a positive dispersion fiber (like SMF-28 fiber), then the blue-shifted components of the pulse will have a larger group velocity and the red-shifted components will have a smaller group velocity. The result will be that the pulse will broaden and significant chirp-induced power penalty will be observed since intersymbol interference will occur. However, if the pulses are transmitted over a negative dispersion fiber then the blue-shifted components of the pulse will have a smaller group velocity and the red-shifted components will have a larger one. The result in this case will be, to some extent, pulse compression and significant transmission performance improvement is expected. Based on these considerations, MetroCor fiber was designed to have negative dispersion to take advantage of the positive chirp characteristics of DMLs, to increase the transmission distance to more than 300 km at 2.5 Gb/s, and to more than 200 km at 10 Gb/s [11].

<sup>1</sup>The opposite will happen for transmitters with negative chirp parameters (as can be the case with externally modulated lasers)

In this paper, it will be shown in detail using both experimental and theoretical results that this specialty fiber can outperform the fibers with conventional dispersion characteristics for Metro area applications. Our studies are focused in the 1310- and 1550-nm wavelength regions, since 1400-nm devices are not commercially available. Results for the performance of MetroCor fiber are shown when all different kinds of transmitters are used (DMLs for 2.5 Gb/s and EA-DFBs, as well as MZ for 10 Gb/s). However, the study is more in-depth for the case DML transmitters. We show that MetroCor fiber can facilitate signal transmission well beyond the conventional 80 to 100 km dispersion limit of directly modulated lasers at 2.5 Gb/s, and electroabsorption modulator integrated DFB laser at 10 Gb/s. It will be shown that it expands the system capabilities up to more than 200 km in all cases. However, it is beneficial for even smaller distances (i.e., 100–150 km) since, as we will show later on, it provides negative power penalties and offers a useful power margin to the network designer that could be used to relax the specifications of other network elements. Therefore, MetroCor fiber could act as a key enabler for low-cost uncompensated optical networking in the metro area.

The paper is organized as follows: In Section II we will study experimentally and theoretically the transmission performance of DMLs over MetroCor fiber and SMF-28 fiber, Section III will be focused on experimental and theoretical comparisons of the transmission performance of electroabsorption modulated lasers over MetroCor and SMF-28 fibers, Section IV will discuss simulation results for the determination of the maximum achievable transmission distance when external modulated lasers are used, and finally, we present a brief summary and the conclusion of this work. It is worth pointing out that all the comparisons presented in this paper were performed between MetroCor fiber and SMF-28 fiber, but the conclusion holds in all the cases that MetroCor fiber is compared with other fibers that have dispersion characteristics similar to that of SMF-28 fiber.

## II. STUDY OF THE TRANSMISSION PERFORMANCE OF DMLs OVER METROCOR AND SMF-28 FIBERS

### A. Modeling of Directly Modulated Lasers for System Simulation Purposes

The transmission performance of waveforms produced by directly modulated lasers over fibers with different signs of dispersion and also different absolute dispersion values strongly depends on the characteristics of the laser frequency chirp. The chirp  $\Delta\nu(t)$  of a DML is related to the laser output optical power  $P(t)$  through the expression [6]–[9], [13], [14]:

$$\Delta\nu(t) = \frac{\alpha}{4\pi} \left\{ \frac{d}{dt} [\ln(P(t))] + \kappa P(t) \right\} \quad (1)$$

where  $\alpha$  is the linewidth enhancement factor and  $\kappa$  the adiabatic chirp coefficient.

In (1), the first term is a structure-independent “transient” chirp, and the second term is a structure-dependent “adiabatic” chirp [13]. The first term has a significant value during relaxation oscillations. The second term is related to the relaxation

oscillation damping, since it is directly proportional to the gain compression factor ( $\epsilon$ ) [3], [4]. Following the definition by Hinton *et al.* [13], the laser diodes can be classified according to their chirp behavior into three broad categories. The two extreme categories are namely the adiabatic- and transient-chirp dominated DMLs. The third category includes the lasers that possess both adiabatic and transient chirp and cannot be classified into the other two. A definition of transient and adiabatic chirp dominated lasers will be reattempted in the present text for clarity reasons. Transient-chirp dominated laser diodes exhibit significantly more overshoot and ringing in output power and frequency deviations. The frequency difference between steady-state ones and zeros is relatively small. Adiabatic-chirp dominated laser diodes exhibit damped oscillations and large frequency difference between steady-state ones and zeros. The transient chirp component, which is always present, will be “masked” by the adiabatic one (this means that the adiabatic chirp term will be larger than the transient chirp).

Several studies have focused on the theoretical analysis of the impact of the frequency chirp on the system performance [8], [9], [13]. However, all the studies have been focused on transmission over transmission fibers with positive dispersion. Studies for the impact of the chirp characteristics in the negative dispersion regime have been performed in the case of transmission systems with dispersion compensating modules [15], but no systematic study has been performed over transmission fibers having negative dispersion. In the following, it will be shown that transient-chirp dominated lasers perform better over negative dispersion fibers than adiabatic-chirp dominated lasers. The transient component of the chirp improves significantly the transmission performance over negative dispersion fibers.

Computer simulations are useful in order to predict the system behavior at the design stage. The decision on the choice of the characteristics of the transmission fiber (i.e., absolute value of dispersion and its sign) for Metro applications should first be determined through simulations. The model that the designer should select and the simulation parameters involved in it should be sufficiently accurate and representative of the majority of commercial available DMLs, so that useful conclusions on the design and performance of the real system will be obtained. Many laser models exist in the literature, each having its own advantages and disadvantages [16]–[19]. However, it has been acknowledged that using the rate equations-based model the laser dynamics can be evaluated sufficiently accurately [8], [9]. Knowledge of the parameters of the model for representative simulations of the system performance is mandatory. Many works have been published during the recent years dealing with the extraction of the rate equation parameters [20]–[22]. To our knowledge, it is not possible to determine experimentally with a single measurement each one of the actual rate equation parameters from a packaged device. It is only possible to determine through measurements, combinations of the parameters, and a limited set of the actual rate equations parameters [20]. In the previous studies [20]–[22], the chirp waveforms, which mainly determine the transmission performance of the DMLs, were either not measured or not used for extraction of chirp related parameters. In addition, in the majority of the previous studies, the validity of the

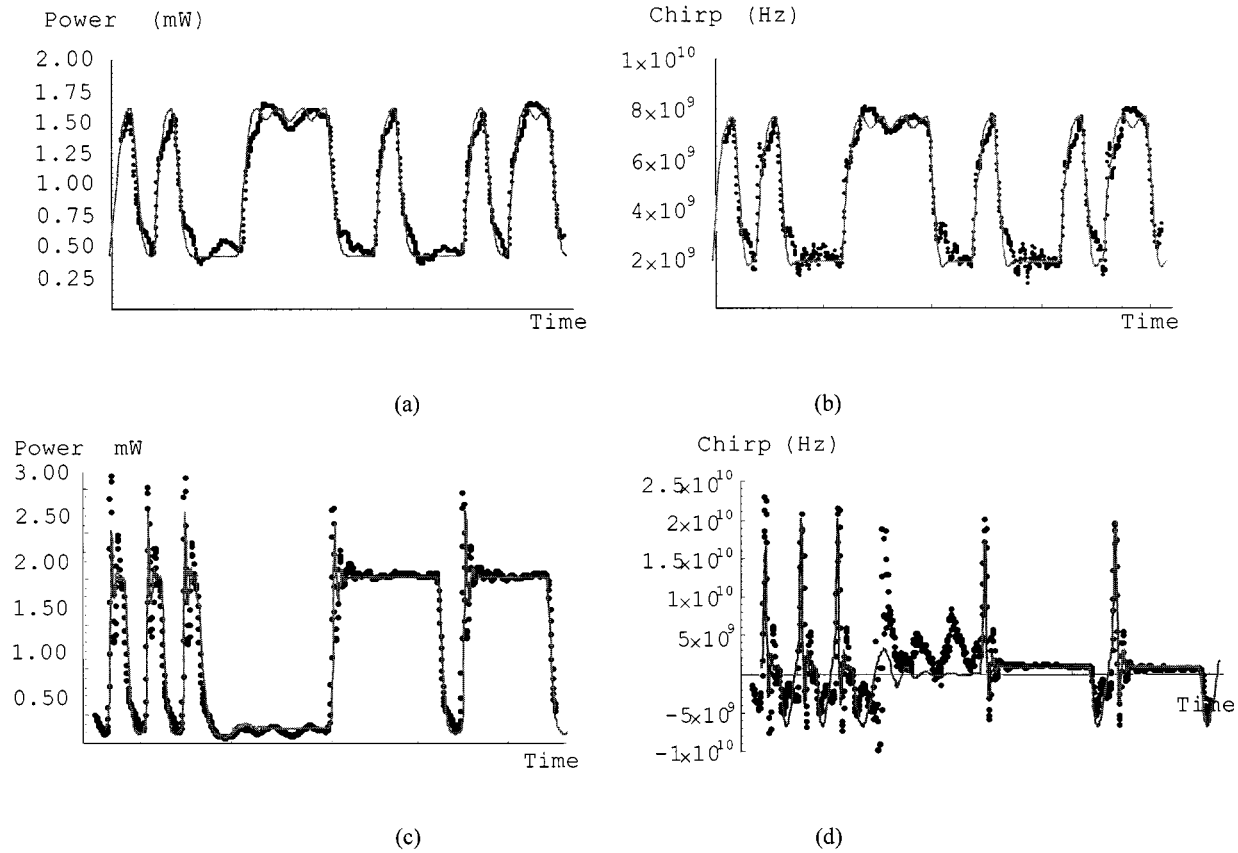


Fig. 3. Measured (dots) and simulated (lines) power (a) and chirp (b) waveforms for two different 2.5-Gb/s DMLs. Upper row: adiabatic chirp dominated DML. Bottom row: Transient chirp dominated DML.

model and the extraction procedures were verified mainly by comparison of measured and simulated intensity modulation (IM) power waveforms. For the purpose of our study, we developed experimental extraction procedures to determine the key combinations of rate equation parameters. Parameters related to the chirp characteristics, in contrast to the previous studies, were extracted directly from chirp measurements. The parameter extraction procedures are based on fitting the measured results of the P-I curve [20], [21], the IM frequency response [20], [21] and the power and chirp waveforms. The details of the parameter extraction procedures will be presented elsewhere [23].

Our parameter extraction procedures were applied to the characterization of various DMLs from different vendors. All DMLs were rated for less than 2-dB chirp-induced power penalty for a dispersion·distance product of 1800 ps/nm, and for an extinction ratio (ER) larger than 8.2 dB at an average optical power of 1 mW. Two of the DMLs presented extreme behaviors. One was strongly adiabatic chirp dominated (DML-1) and another was strongly transient chirp dominated (DML-2). The values of the extracted parameters for the two DMLs are shown in Table I. The relation of the extracted parameters with the actual rate equation parameters is also shown in the table. For the definition of the parameters see the table caption or [20].

Some overall results indicating the robustness of the extraction procedures and the validity of the rate equations-based laser model are presented in Fig. 3, where the measured and simulated power and chirp waveforms are compared. The simulation

TABLE I

Parameter	Units	DML-1	DML-2
$\alpha$	-	2.2	5.6
$\kappa = \frac{2\Gamma}{\eta h \nu V} \cdot \epsilon$	Hz W <sup>-1</sup>	$28.7 \cdot 10^{12}$	$1.5 \cdot 10^{12}$
$K = 4\pi^2 \left( \tau_p + \frac{\epsilon}{g_0} \right)$	ps	518	420
$\tau_c$	ns	0.374	0.256
$\Phi = \frac{2e\lambda}{hc\eta}$	A/W	16.35	14.48
$I_m = \frac{eV}{\tau_c} \left( N_0 + \frac{1}{\Gamma g_0 \tau_p} \right)$	mA	4.66	17.34
$I_s = \frac{\beta e V}{\Gamma g_0 \tau_c \tau_p}$	A	$11.2 \cdot 10^{-8}$	$7.3 \cdot 10^{-8}$
$\Gamma g_0 / eV$	Hz <sup>2</sup> /A	$1.848 \cdot 10^{23}$	$1.08 \cdot 10^{23}$

Extracted parameter values of each DMLs. (Definition of symbols:  $\lambda$  is the emission wavelength,  $\nu$  is the optical frequency,  $\eta$  is the quantum efficiency,  $\Gamma$  is the confinement factor,  $N_0$  is the carrier density at transparency,  $\beta$  is the fraction of spontaneous emission noise coupled into the lasing mode,  $g_0$  is the differential gain coefficient,  $\epsilon$  is the nonlinear gain compression factor,  $\tau_p$  is the photon lifetime,  $\tau_c$  is the carrier lifetime,  $V$  is the volume of the active layer,  $e$  is the electron charge,  $h$  is the plank's constant,  $c$  is the speed of light in vacuum and  $\alpha$  is the linewidth enhancement factor.)

conditions were adjusted to the experimental ones. The simulations and the experiments show that DML-1 is clearly adiabatic chirp dominated as can be seen from the chirp waveform [see Fig. 3(b)]. The transient chirp has been completely masked by the adiabatic chirp component. A very good damping of the re-

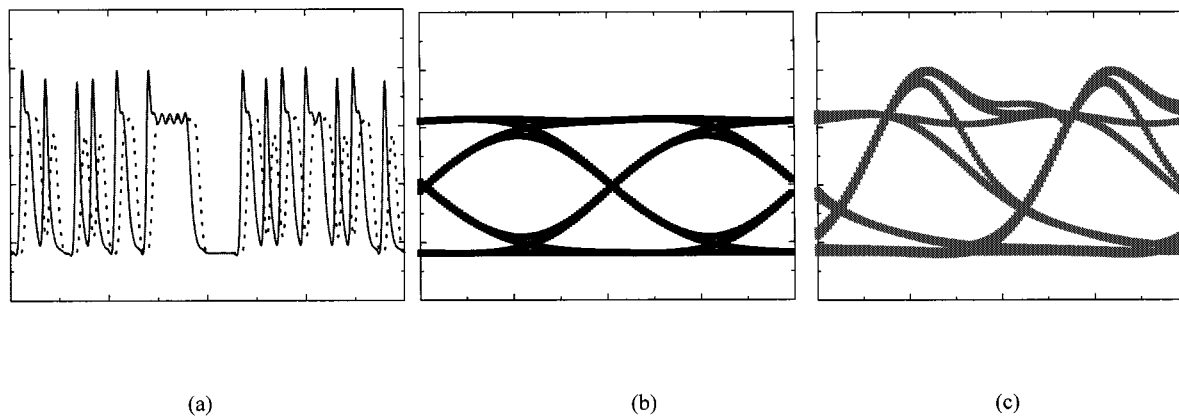


Fig. 4. Simulated results for the transmission performance of a 2.5-Gb/s adiabatic chirp dominated transmitter over SMF-28 fiber where the dispersion is positive. (a) Bit sequences before (dotted line) and after (solid line) transmission over 300-km SMF-28 fiber. (b) Eye pattern at the transmitter side. (c) Eye pattern at the receiver side.

laxation oscillations on the 1s and the 0s is also evident. Isolated 1s have a power overshoot that appears at the trailing edge of the pulse and not at the leading edge as it is the usual case. This behavior is attributed to the characteristics of the parasitics for this DML. DML-2 [see Fig. 3(c), (d)] is transient chirp dominated. The adiabatic chirp component is significantly lower than the transient chirp component. The peak-to-peak chirp is approximately 30 GHz, a value that results in considerably broad spectrum, and consequently an increased dispersion penalty for transmission over positive dispersion fibers is expected. The power waveform shows a large power overshoot on the 1s, while the undershoot on the 0s is rather small. The damping of the relaxation oscillations on both the 1s and the 0s is not fast. The comparison between simulations and experiments is exceptional, except for the regions that correspond to low power levels (0s). For such low power levels the chirp measurements are not accurate, which explains to some extent, the discrepancies between the fitted simulation results and the measurements.

The simulation results for both the power and chirp waveforms for both DMLs are in very good agreement with the experiment. Therefore, we are confident that we have a sufficiently accurate representation of DMLs, and we can perform simulations using the rate equations DML model that will help us identify the characteristics of the fiber for best transmission performance in metropolitan area applications.

#### B. Transmission Simulations of DML With Different Chirp Characteristics Over SMF-28 and MetroCor Fibers

In this section, we employ a heightened understanding of chirp characteristics of directly modulated lasers to address the dispersion-induced deformation on the transmitted waveforms. Both pulse shape and chirp characteristics are important for the determination of the transmission performance of DMLs. Analysis of these characteristics can give us an insight on the performance of DMLs and an understanding of the various features of the experimentally observed eye patterns.

In order to study the transmission performance at 2.5 Gb/s of DMLs presenting extreme behaviors (either adiabatic or transient) over fibers with positive or negative dispersion, we performed a set of simulations. The DMLs were modeled using the

rate equation model [8], [9] and the experimentally extracted parameters (Session II.A). The results of the simulations revealed the features of the interaction of chirp with the fiber dispersion and pulse shape in the cases of transmission of signals produced from adiabatic or transient chirp dominated transmitters over positive or negative dispersion fibers.

In Fig. 4, the transmitted and received bit patterns and eye diagrams are shown for the case of an adiabatic chirp dominated transmitter (DML-1) before and after transmission over 300 km of SMF-28 fiber (the fiber attenuation in all the simulations was set to zero). It is obvious from the simulations that the effects on the received bit pattern of the interplay of the chirp with the dispersion are (a) the formation of an intense peak either in isolated 1s or in the first “1” of a series of 1s and (b) an increased trailing tail of the pulses. The resulted received eye is deformed but not severely closed.

In Fig. 5, the transmitted and received bit patterns and eye diagrams are shown for the case of the adiabatic chirp dominated transmitter before and after transmission over 300 km of MetroCor fiber. From the simulations, it is evident that the effects on the received bit pattern from the interplay of the chirp with the dispersion have been reversed in this case in comparison with the case of transmission over positive dispersion fiber. The formation of the peak appears now on the last “1” of a series of 1s and the leading tail of the pulses has increased. The effects are not so pronounced because MetroCor fiber has a small absolute value of dispersion, which is less than half of that for SMF-28 fiber. The received eye after 300 km is slightly deformed.

In Fig. 6, the transmitted and received bit patterns and eye diagrams are shown for the case of a transient chirp dominated transmitter before and after transmission over 300 km of SMF-28 fiber. As we can see in Fig. 6, the main effect on the received bit pattern of the interplay of the chirp with the dispersion in this case is the significant intersymbol interference. The received eye pattern is severely closed.

In Fig. 7, the transmitted and received bit-patterns and eye diagrams are shown for the case of the transient chirp-dominated transmitter before and after transmission over 300 km of MetroCor fiber. From the simulation, results it can be observed

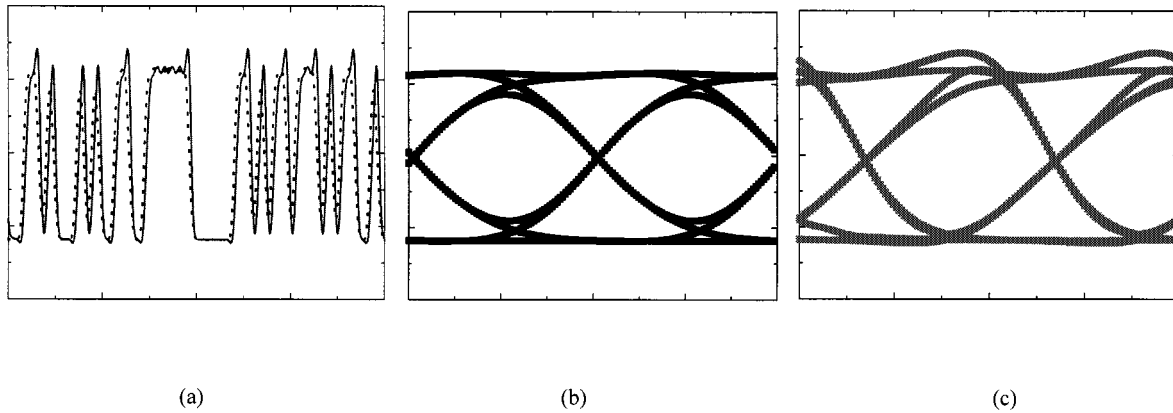


Fig. 5. Simulated results for the transmission performance of a 2.5-Gb/s adiabatic chirp dominated transmitter over MetroCor fiber where the dispersion is negative. (a) Bit sequences before (dotted line) and after (solid line) transmission over 300-km MetroCor fiber. (b) Eye pattern at the transmitter side. (c) Eye pattern at the receiver side.

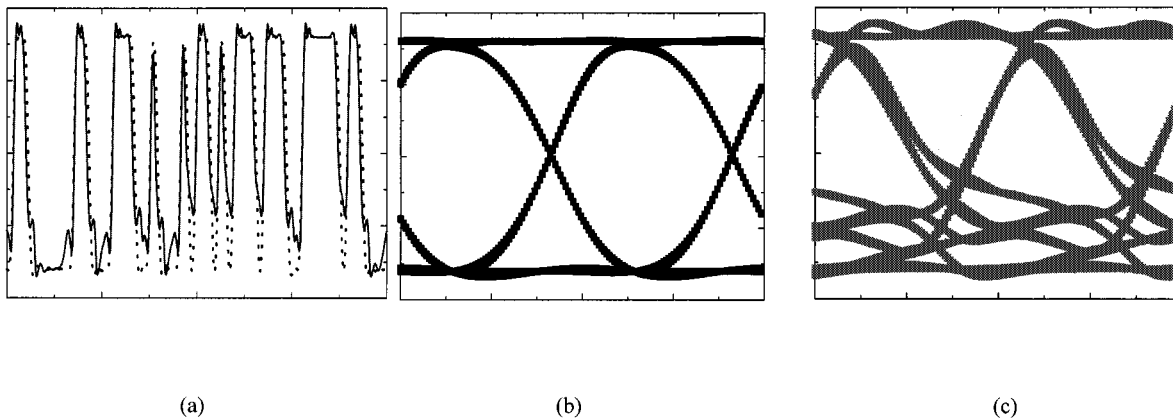


Fig. 6. Simulated results for the transmission performance of a 2.5-Gb/s transient chirp dominated transmitter over SMF-28 fiber where the dispersion is positive. (a) Bit sequences before (dotted line) and after (solid line) transmission over 300-km SMF-28 fiber (b) Eye pattern at the transmitter side. (c) Eye-pattern at the receiver side.

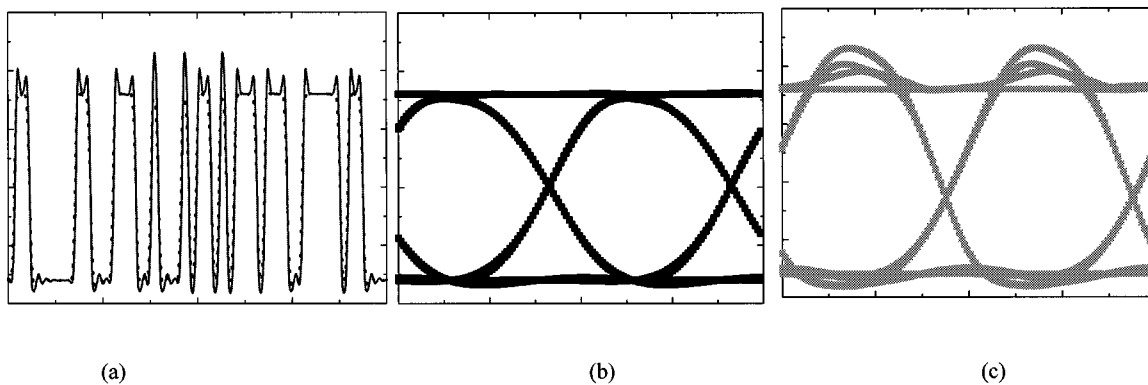


Fig. 7. Simulated results for the transmission performance of a 2.5-Gb/s transient chirp dominated transmitter over MetroCor fiber where the dispersion is negative. (a) Bit sequences before (dotted line) and after (solid line) transmission over 300-km MetroCor fiber. (b) Eye pattern at the transmitter side. (c) Eye-pattern at the receiver side.

that the only effects on the received bitpattern from the interplay of the chirp with the dispersion is the formation of some peaks on top of the 1s. The received eye pattern after 300 km is completely open.

All the features of the received waveforms can be easily explained by considering the interaction of the laser chirp and pulse shape with the fiber dispersion [8], [24], [25]. In fact,

knowledge of the power and chirp waveforms at the output of the DFB laser can be used to predict the shape of the received eye pattern. Conversely, the shape of the received eye can be used to infer the chirp characteristics of the laser. In Fig. 8, the power and chirp waveforms of transient and adiabatic chirp dominated DMLs, before and after transmission over fibers with different dispersion signs is shown in a simplified way. Based on this

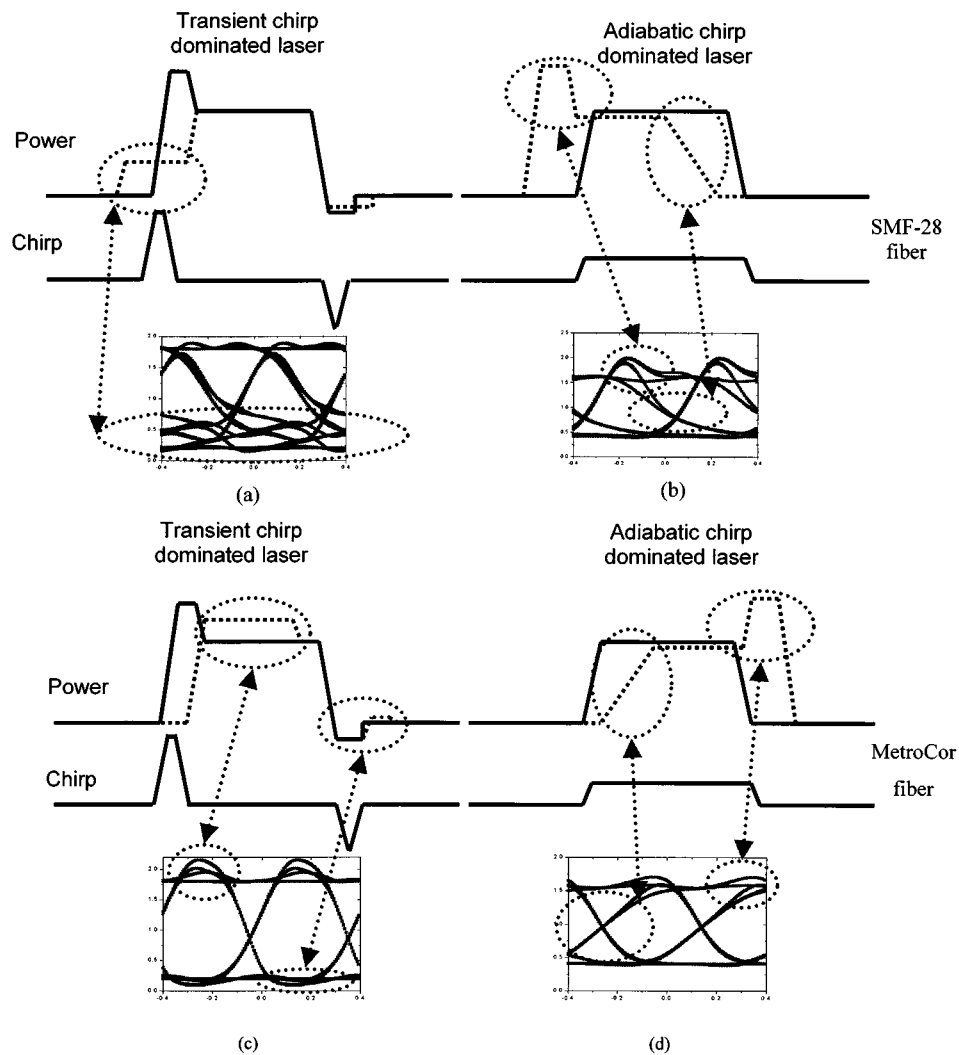


Fig. 8. Schematic explanation of the interaction of the chirp with the dispersion and the pulse shape. (a), (b) Transmission over fiber with positive dispersion (i.e., SMF-28 fiber) and (c), (d) Transmission over fiber with negative dispersion (i.e., MetroCor fiber). Solid lines represent the shapes before transmission, while the dotted lines after transmission.

figure, a qualitative explanation of the shape of the received eyes depending on the chirp characteristics of the DML is presented.

In the case of transient chirp dominated laser [see Fig. 8(a)], the leading edge of the pulse is blue-shifted relative to the main portion of the pulse, while the trailing edge is red-shifted (see the chirp waveform). In addition, the leading edge of the pulse has higher power (overshoot) than the main portion of the pulse. The blue-shifted chirped portion advances relative to the main portion of the pulses for transmission over positive dispersion fibers. This effect will result in pulse spreading (Fig. 8(a) dotted line) and intersymbol interference will occur. As a consequence the eye pattern after transmission will be severely closed. On the other hand, the blue-shifted leading edge of the pulse will compress the pulses through transmission over negative dispersion fiber (MetroCor fiber) and the eye will look perfectly open [see Fig. 8(c)].

In the case of an adiabatic chirp dominated laser, where the transient chirp has been completely “masked” by the adiabatic term [see Fig. 8(b)], there will be a distinct separation between the frequency of the 1s and the 0s. The frequency of the 1s will

be larger than the frequency of 0s (blue shift). Since the extinction ratio has a finite value power will be present on the 0s. Therefore, the result of the interplay of the dispersion with the specific chirp characteristics will result in a high intensity spike at the front of the pulses and a trailing tail-end for transmission over positive dispersion fiber. Exactly the opposite effects will take place for transmission over a negative dispersion fiber [see Fig. 8(d)]. In the case of an adiabatic chirp dominated DML, the absolute value of the dispersion (and not its sign) will play the major role in the transmission performance. The eye corresponding to transmission over SMF-28 fiber will be more distorted than that corresponding to transmission over MetroCor fiber because of the larger absolute value of the dispersion. The different dispersion sign will just affect the asymmetry of the eye diagram, as it is obvious from the results of Fig. 8(b) and (d).

Clearly, all the above results show that the MetroCor fiber outperforms the SMF-28 fiber in both cases of adiabatic and transient chirp dominated lasers because of its characteristics (i.e., the negative dispersion and the reduced absolute value of

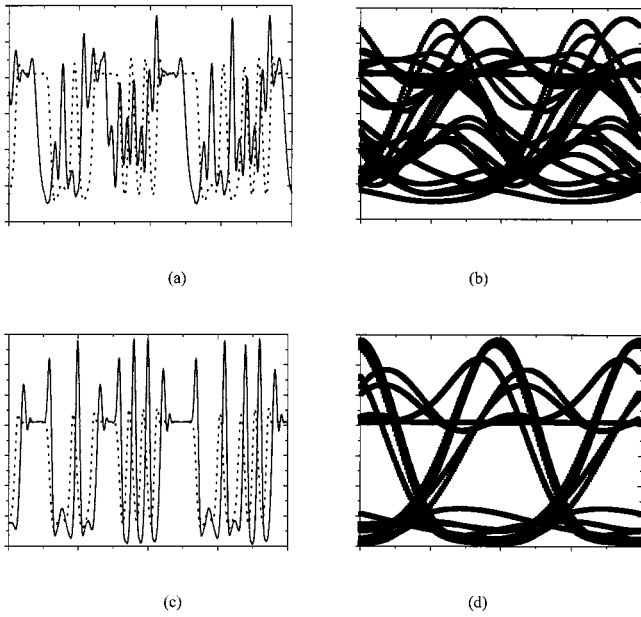


Fig. 9. Simulated results for the transmission performance at 10 Gb/s of a transient chirp dominated transmitter over 120 km of either SMF-28 or MetroCor fibers. (a), (c) Bit sequences before (black) and after (red) transmission. (b), (d) Eye patterns at the receiver for the cases of SMF-28 and MetroCor fibers, respectively.

dispersion). However the benefit from the use of MetroCor fiber is shown to be more pronounced in the case of transient chirp dominated DMLs than in the case of adiabatic chirp dominated ones. This statement is confirmed also with a small signal analysis presented in Appendix A.

### C. Transmission Simulations of 10-Gb/s DML Waveforms

In order to have acceptable transmission performance with 10-Gb/s signals produced by 1550-nm DMLs over at least 40–50 km of SMF-28 fiber, special laser designs should be developed that will reduce the transient chirp and enhance the adiabatic chirp [26]. However, using conventional laser designs at 10 Gb/s (where the pulse rise- and fall-times are small) the transient chirp [first term in (1)] becomes even more pronounced than 2.5 Gb/s. Therefore, transmission of intensity modulated OOK optical signal even over 10–20 km of positive dispersion fiber will result in significant power penalties. The use of a negative dispersion fiber will dramatically enhance the capabilities of 10-Gb/s directly modulated lasers. It is expected that at 10 Gb/s, the improvement in the transmission performance over MetroCor fiber relative to that over SMF-28 fiber will be more pronounced than that at 2.5 Gb/s. In order to prove our expectation, we performed some transmission simulations. The laser parameters were selected to have the same values like those measured for a 2.5-Gb/s DML (DML-1). DML-1 presents strongly adiabatic chirp behavior at 2.5 Gb/s (see Section II-A), but at 10 Gb/s, the transient chirp is not masked any more by the adiabatic chirp component and is much more significant. In Fig. 9, the received bit patterns and eye patterns after transmission over 120 km of SMF-28 fiber [see Fig. 9(b)] or MetroCor [see Fig. 9(d)] fibers are presented. The results of the transmission simulation clearly reveal the potential benefit from the use of MetroCor fiber with 10-Gb/s

TABLE II  
VALUES OF LASER RATE EQUATION PARAMETERS (FROM [26])

Parameter	Units	Description	Value
$\tau_c$	ns	Carrier lifetime	3.17
V	m <sup>3</sup>	Active volume	3.60E-17
$\beta$		Spontaneous emission fraction	1.00E-03
$\Gamma$		Confinement factor	0.2408
$a_0$	m <sup>2</sup>	Differential gain	3.34E-20
$\tau_p$	ps	Photon lifetime	2.6
$n_0$	1/m <sup>3</sup>	Carrier density at transparency	2.00E+24
$\lambda$	mm	Wavelength	1.3
R		Power reflectivity	0.158
L	mm	Length	0.3
$\epsilon$	m <sup>3</sup>	Nonlinear gain compression factor	2.00E-23
$n_g$		group refractive index	4
$\alpha$		Linewidth enhancement factor	6
$I_0$	mA	Current for 0	6.5
$I_1$	mA	Current for 1	18

TABLE III  
RANGES THAT THE PARAMETERS OF TABLE II WERE VARIED FOR THE SIMULATIONS

Parameters	Units	Description	Range
$\tau_c$	ns	Carrier lifetime	0.5-3.5
V	e-17 m <sup>3</sup>	Active volume	2.0-10.0
$\alpha_0 x v_g$	e-12 m <sup>2</sup> /s	Differential gain	1.0-9.0
$n_0$	e24 1/m <sup>3</sup>	Carrier density at transparency	0.5-2.5
L	mm	Length	0.2-0.4
$\epsilon$	e-23 m <sup>3</sup>	Nonlinear gain compression factor	1.0-9.0
$\alpha$		Linewidth enhancement factor	3.0-9.0

DMLs. The eye pattern after transmission over 120 km is clearly open. These encouraging simulation results for 10-Gb/s 1550-nm DMLs await experimental confirmation. It should be noted that the currently commercial available 10-Gb/s DMLs can achieve transmission distances of 10 km over SMF-28 fiber when the extinction ratio is larger than 8.2 dB.

### D. Transmission Simulations of a Large Population of DMLs Over SMF-28 and MetroCor Fibers

It is of interest to investigate if the MetroCor fiber will perform better than the SMF-28 fiber for a large population of DMLs with a variety of different modulation characteristics. A way of producing output waveforms with different characteristics is to vary the laser parameters. In the rate equations-based model, many independent parameters are involved, see (14). Obviously, it is very difficult to investigate exhaustively the impact of each one of the parameters on the transmission performance of the DFB lasers. Also, it is not possible to vary the values of all the parameters since the number of the different combinations will be very large. Therefore, in the present study only seven parameters of the DFB laser were varied around the values given in Table II, [27]. The selected parameters are among the most influential for the transmission performance [13]. The ranges that we assumed are given in Table III. Each range is sampled at the end points and the middle, yielding a population of 2187 lasers.

In the simulations, the modulating current was composed of 2.5-Gb/s raised-cosine current pulses with rise and fall times of 100 ps. Bias currents for the ones and zeros are chosen to

achieve 1-mW average optical power and 10-dB extinction ratio for each laser. Under these driving conditions, 31.5% of the lasers presented ringing that resulted in larger than 0.5 dB back-to-back penalty, while 11% of the generated laser population presented power ringing that causes more than 1-dB back-to-back eye closure power penalty. In Fig. 10, we give as an example the eye patterns of simulated lasers experiencing 0.5-, 1-, and 3-dB eye-closure penalty, together with a typical experimentally measured eye pattern of a commercially available DML. It can be seen that the typical experimentally measured eye pattern looks more like the eye patterns of Fig. 10(a), (b) than that of Fig. 10(c), which is not representative of commercially available DMLs.

For the transmission simulations, the fiber was modeled as an all-pass filter with quadratic phase [28]. Nonlinear effects were ignored due to the small transmitted powers and the short distances involved in typical metropolitan networks. The receiver optical filter was assumed to be a third-order Butterworth filter. The photodiode was modeled as a square law detector followed by a fourth-order Bessel electric low-pass filter [29]. The chirp-induced penalty was estimated by calculating the amount of eye degradation at the output of the receiver [28].

In Fig. 11, the power penalty for each one of the generated samples of DMLs is shown as a function of the transmission distance over MetroCor fiber (black dotted lines) and SMF-28 fiber (gray solid lines). In the simulations the transmission wavelength is chosen to be 1528.77 nm, which is the lower end of the *C*-band. This represents the best case scenario for the transmission over SMF-28 fiber, and the worst-case scenario for MetroCor fiber. From the laser population, we rejected first all lasers with a back-to-back penalty larger than 1 dB [see Fig. 11(a)], and then the lasers having larger than 0.5-dB penalty [see Fig. 11(b)]. It is obvious from these results more lasers perform better (having smaller than 2-dB eye-closure penalty) over a certain distance of MetroCor fiber than over SMF-28 fiber.

In Fig. 12, the overall exhaustive simulation results are shown for the two fiber types. The fraction of the initial acceptable laser population that after fiber transmission has less than 2-dB dispersion-induced penalty is plotted as a function of distance. In the initial acceptable laser population, we included all lasers having (a) a back-to-back penalty smaller than 1 dB, and (b) a dispersion · length product (dispersion tolerance) larger than 1000 ps/nm. The results suggest that at least 94% of the remaining lasers can go through 300 km-D NZDSF, while at most 43% of the remaining lasers can go through 300 km of SMF-28 fiber. These numbers are based on the assumption that the probability of occurrence of each DFB semiconductor laser in the simulated population is the same. It also should be noted that these results would change if the model parameters will change. However, the results clearly demonstrates in a qualitatively way that MetroCor fiber has a superior performance in comparison to SMF-28 fiber for a large variety of DMLs.

#### E. Experimental Comparison of Positive and Negative Dispersion Tolerance

In order to experimentally compare the tolerance of directly modulated DFB lasers to positive and negative dispersion, we

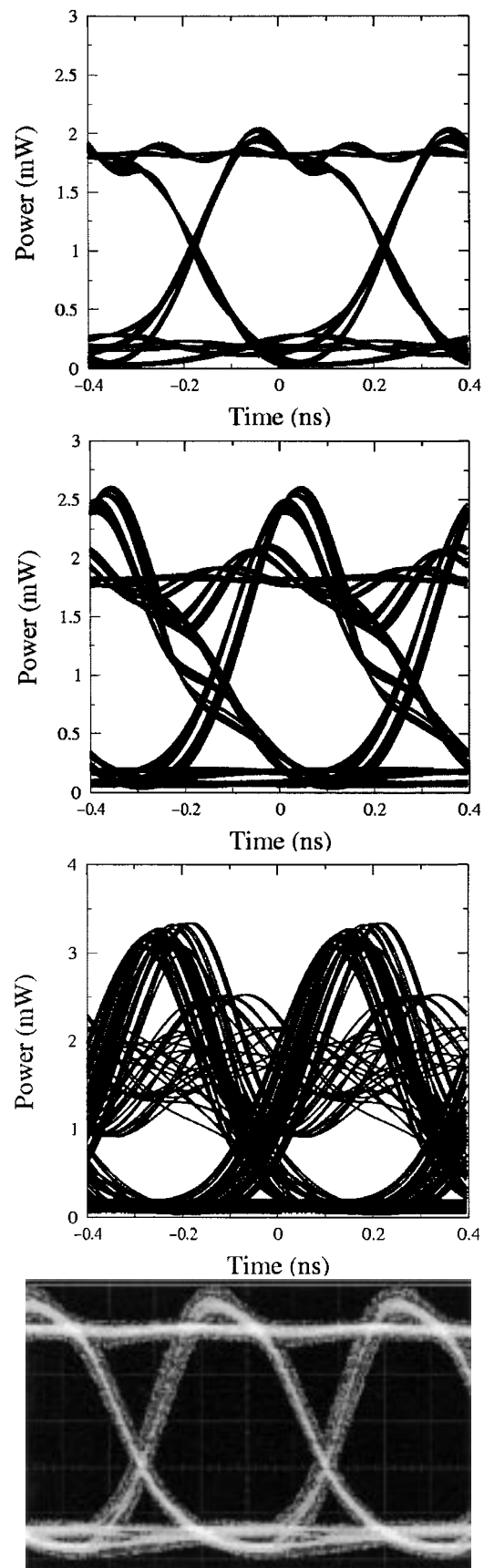
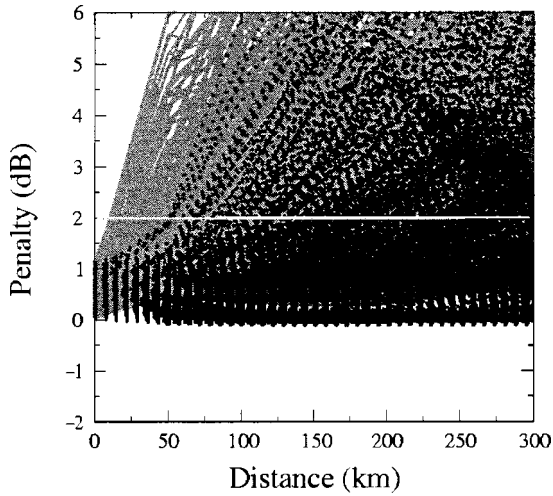
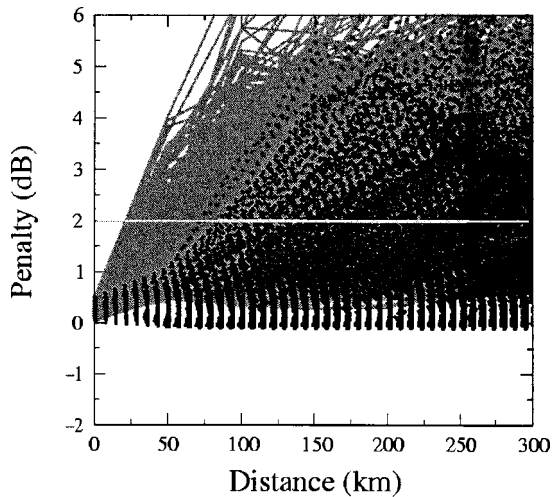


Fig. 10. Simulated eye patterns for 2.5-Gb/s lasers experiencing (a) 0.5, (b) 1, and (c) 3-dB eye closure penalty. (d) Typical experimentally measured filtered eye pattern is shown.



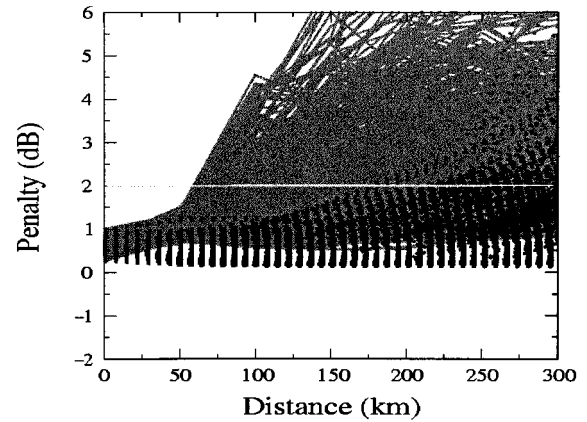
(a)



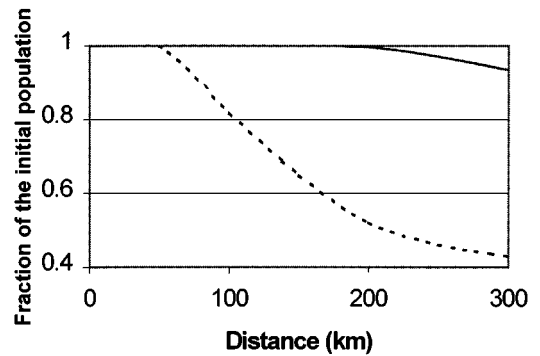
(b)

Fig. 11. Power penalty for each one of the generated simulated 2.5-Gb/s DMLs versus the transmission distance over MetroCor (black dotted lines) and SMF-28 (gray solid lines) fibers. (a) 1938 lasers having smaller than 1-dB back-to-back penalty. (b) 1497 lasers having smaller than 0.5-dB back-to-back penalty. The horizontal straight line indicates the 2-dB penalty limit.

measured the performance of different DFB lasers over positive dispersion using SMF-28 fiber and over negative dispersion using MetroCor fiber. A total of five different commercially available directly modulated DFB lasers (DML-1, -2, -3, -4, -5) from three different vendors were measured. All lasers had rated dispersion tolerances for positive dispersion fibers between 1440 and 3000 ps/nm for OC-48 transmission. The DMLs were first characterized in terms of the chirp characteristics. DML-1 is an adiabatic chirp dominated laser (is the same DML that studied as DML-1 in Session II-A), while DML-5 is transient chirp dominated (the same DML that studied as DML-2 in Session II.A). DML-2, -3, -4 had large transient chirp (not larger than DML-5), but also a large adiabatic chirp component (however, much smaller than DML-1). The lasers were modulated at 2.5 Gb/s with a  $2^{31} - 1$  pseudorandom bit sequence (PRBS). Erbium-doped fiber amplifiers (EDFAs) with a noise figure of about 6–7 dB were used to compensate for the fiber losses. Variable optical attenuators (VOAs) were placed before and after each amplifier to set the optical signal power level launched into



(a)



(b)

Fig. 12. (a) Power penalty for each one of the generated simulated 2.5-Gb/s DMLs versus the transmission distance over MetroCor (black dotted lines) and SMF-28 (gray solid lines) fibers for 1100 lasers having a back-to-back penalty smaller than 1 dB and a Dispersion/Length product rating larger than 1000 ps/nm. (b) Simulated yield of those DMLs to propagate through MetroCor fiber and SMF-28 fiber with less than 2-dB penalty.

each fiber span to 0 dBm, and the input signal power level into each EDFA to  $-26$  dBm. An optically preamplified receiver was used to detect the optical signal after propagation through the fiber.

The receiver sensitivity at a bit-error rate (BER) of  $10^{-9}$  and the  $Q$ -factor performance measure for each of the five lasers are plotted as a function of dispersion in Fig. 13. The results are plotted at different extinction ratios for each laser. DMLs from -2 to -5 showed substantially greater tolerance to negative dispersion than to positive dispersion. This performance enhancement is dependent upon the extinction ratio. The adiabatic chirp dominated DML-1, however, showed no significant difference between performance over positive or negative dispersion fiber.

The maximum dispersion tolerance for each of the five lasers is shown below in Table IV. Here, the dispersion tolerance is defined as the maximum dispersion for which a  $Q$ -factor greater than 9 dB<sup>2</sup> (i.e., BER  $< 10^{-15}$ ) was achieved. The extinction

<sup>2</sup>We define  $Q$  (dB) =  $10 * \text{Log}[Q(\text{linear})]$ , although the definition  $Q$  (dB) =  $20 * \text{Log}[Q(\text{linear})]$  is more often used in the literature.

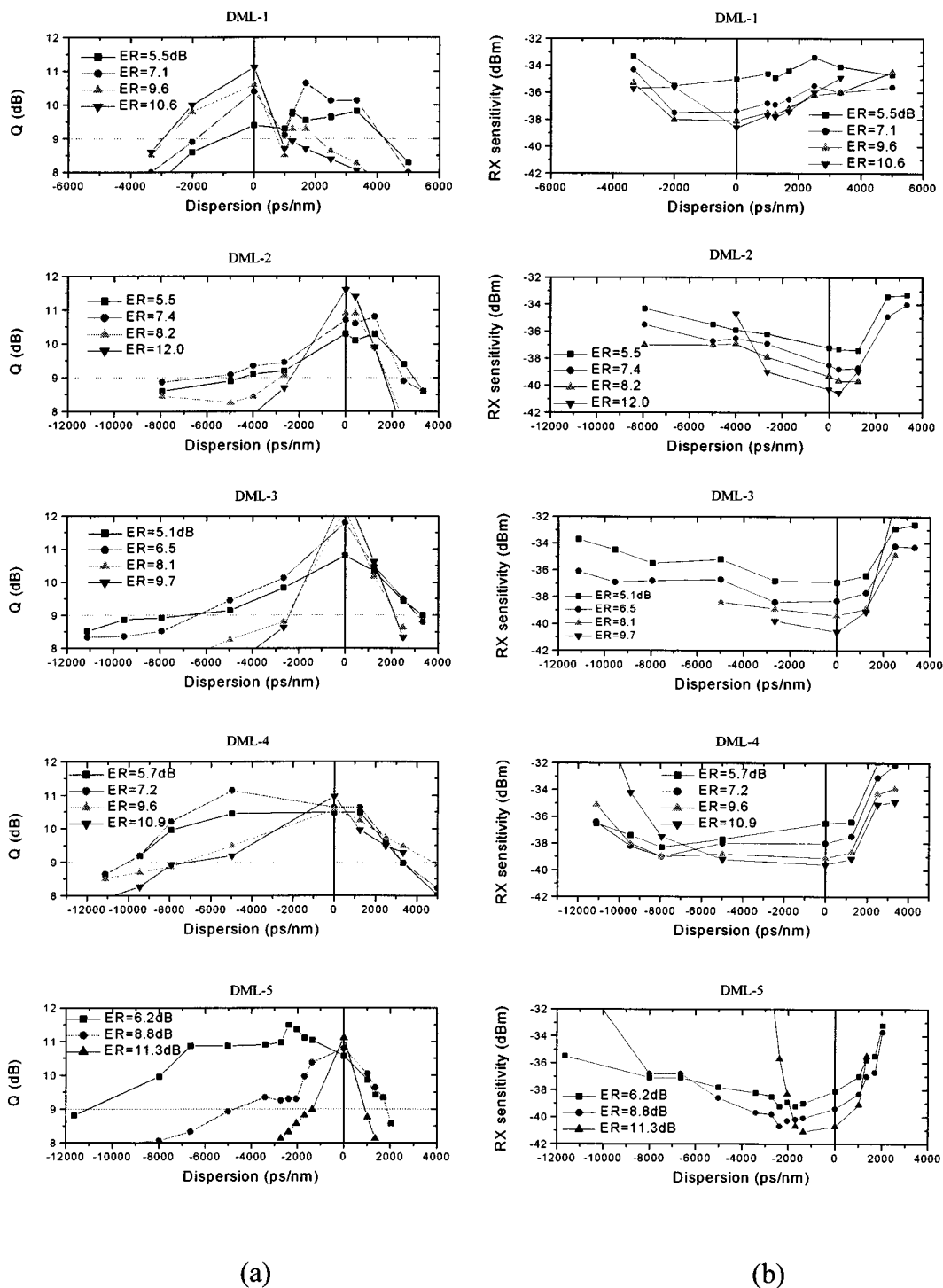


Fig. 13. Measured transmission performance in terms of  $Q$ -factor and (a) receiver sensitivity of (b) five 2.5-Gb/s directly modulated lasers over positive and negative dispersion fibers. (Abbreviations used: ER = extinction ratio, Rx = Receiver.)

ratio at which this is achieved is also shown. It is obvious that the DMLs having large transient chirp (DMLs 2 to 5) are favored in terms of  $Q$ -factor performance by small extinction ratios (the  $Q$ -penalty is smaller for small extinction ratios). The adiabatic chirp dominated DML-1 is favored by small extinction ratios in the case of maximum positive dispersion tolerance, but in the case of maximum negative dispersion tolerance is favored by a large extinction ratio. However, in general, small extinction ratios cause increased receiver sensitivity penalties. Therefore, if

we limit ourselves to extinction ratios of more than 8.2 dB, as specified in current SONET specifications [29], [30], the dispersion tolerances achieved are shown in Table V.

Using a negative dispersion fiber gave improvements in absolute dispersion tolerance of typically 100% under optimized bias conditions, and improvements of about 50% under standard SONET drive conditions relative to SMF-28 fiber. The comparisons were performed by considering the value of the dispersion  $\cdot$  length product (dispersion tolerance). How-

TABLE IV  
DISPERSION TOLERANCE OF DMLs AT OPTIMIZED EXTINCTION RATIOS

	Positive Dispersion Tolerance	Negative Dispersion Tolerance	Percent improvement in absolute dispersion tolerance for negative dispersion
DML-1	+4200ps/nm @ ER=5.5dB	-3000ps/nm @ ER=10.6dB	-28%
DML-2	+2900ps/nm @ ER=5.5dB	-6200ps/nm @ ER=7.4dB	114%
DML-3	+3400ps/nm @ ER=5.1dB	-7000ps/nm @ ER=5.1dB	106%
DML-4	+4800ps/nm @ ER=9.6dB	-10000ps/nm @ ER=5.7dB	108%
DML-5	+1800ps/nm @ ER=6.2dB	-11000ps/nm @ ER=6.2dB	511%

TABLE V  
DISPERSION TOLERANCE OF DMLs UNDER SDH/SONET SPECIFIED EXTINCTION RATIOS (LARGER THAN 8.2 dB)

	Positive Dispersion Tolerance	Negative Dispersion Tolerance	Percent improvement in absolute dispersion tolerance for negative dispersion
DML-1	+2100ps/nm	-3000ps/nm	43%
DML-2	+1700ps/nm	-2600ps/nm	53%
DML-3	+2200ps/nm	-2500ps/nm	14%
DML-4	+4800ps/nm	-7300ps/nm	52%
DML-5	+1800ps/nm	-4700ps/nm	161%

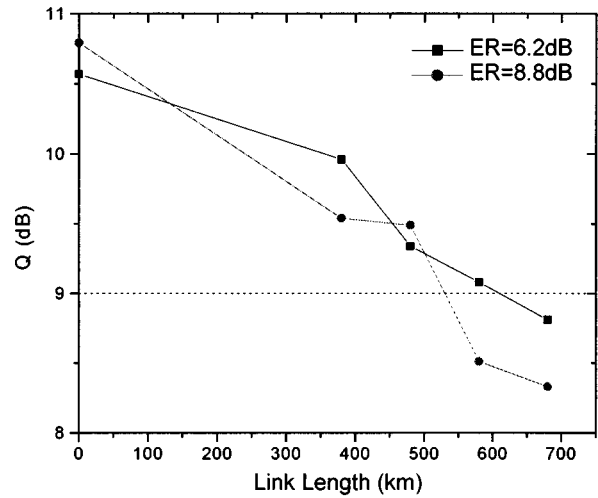
ever, since MetroCor fiber has also smaller absolute value of dispersion, the distance that the signals can be transmitted will be always larger when using MetroCor fiber instead of SMF-28 fiber.

#### F. Performance Over 600 km of MetroCor Fiber

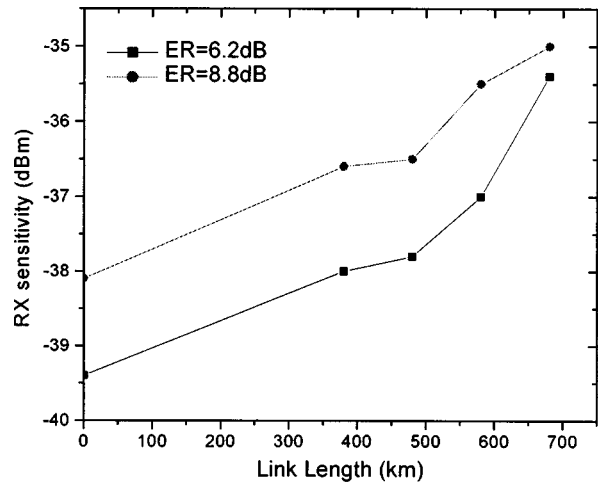
Similar experiments were performed using 600 km of MetroCor fiber. As shown in Fig. 14, error-free transmission ( $BER < 10^{-12}$ ) over 600 km of the negative dispersion fiber with six inline EDFAs could be obtained using a DML rated for 80 km of transmission distance over SMF-28 fiber. Again, this result was achieved with no additional dispersion compensation in the system. This shows that a significant increase in propagation distance is possible when negative dispersion fiber is used in combination with less expensive DMLs in metropolitan systems.

#### G. 32-Channel DWDM System Experiment at 2.5 Gb/s

A fully loaded 32-channel DWDM transmission experiment was also conducted to verify that the MetroCor fiber enables longer uncompensated reach with DMLs [10]. The experimental setup is shown schematically in Fig. 15. The experiments focused on the C-band, where the MetroCor fiber has higher absolute value of dispersion. The channel wavelengths were between 1533.5 and 1558.2 nm with 100-GHz spacing on the ITU-T grid. Optical switches were used to select either 300 km of MetroCor fiber or 300 km of SMF-28 fiber. The experiment used EDFAs, which were optimized for metropolitan DWDM systems, and had a total output power of +14 dBm. The average channel power launched into each fiber span was -3 dBm. The OSNR



(a)



(b)

Fig. 14. Measured performance of DML-5 over various distances of MetroCor fiber for different extinction ratios (a)  $Q$ -factor values and (b) receiver sensitivity.

at the receiver was greater than 23 dB at 0.1-nm bandwidth for all 32 channels.

Fig. 16 shows a comparison of the measured  $Q$ -factors after propagation over 300 km of MetroCor or SMF-28 fibers. As shown by the solid dots in the case of transmission over MetroCor fiber, all 32 channels have a  $Q$  higher than 9 dB, corresponding to a BER lower than  $10^{-15}$ . In the contrast, all of the channels fail after propagation over 300 km of SMF-28 fiber, as shown by the open circles.

The power penalty for achieving a BER of  $10^{-10}$  was also measured and the results are presented in Fig. 17. After 300 km of MetroCor fiber all 32 channels show a negative power penalty (ranging from 0.3 to about 1.5 dB), which essentially means performance improvement when using MetroCor fiber versus the inline case of no fiber. On the other hand, there is a significant power penalty (larger than 4 dB) for those signals that propagate through 300 km of SMF-28 fiber. It is worth pointing out that 24 lasers presented a power penalty larger than 10 dB.

Obviously, the performance difference between MetroCor fiber and SMF-28 fiber is strongly device dependent, as shown

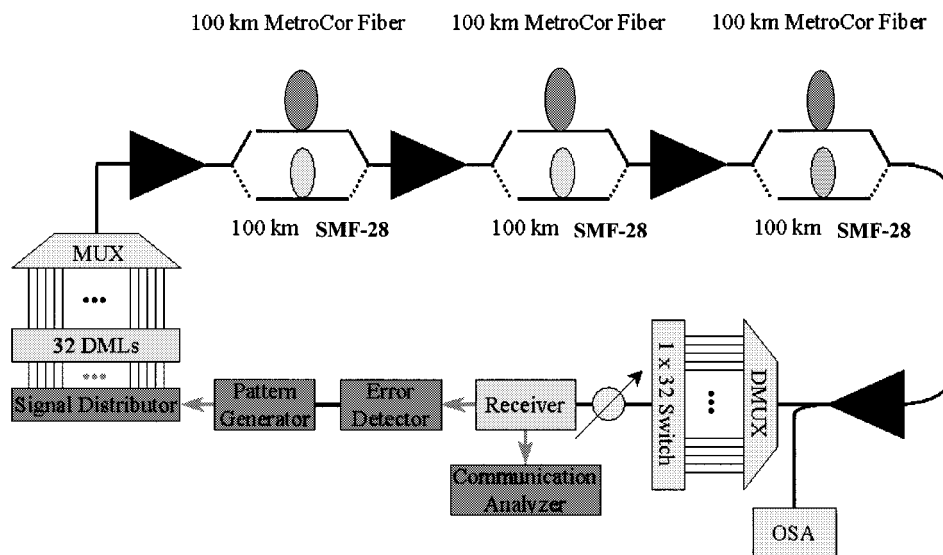


Fig. 15. Experimental setup for comparing the transmission performance over SMF-28 and MetroCor fibers.

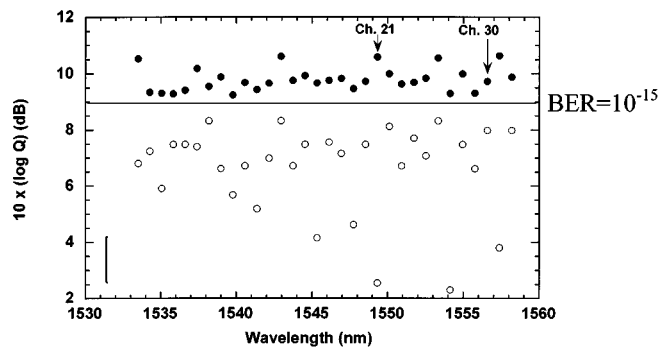


Fig. 16. Comparison of measured  $Q$ -factors after transmission of 32 2.5-Gb/s DMLs over 300 km of MetroCor fiber (open circles) and SMF-28 fiber (solid circles).

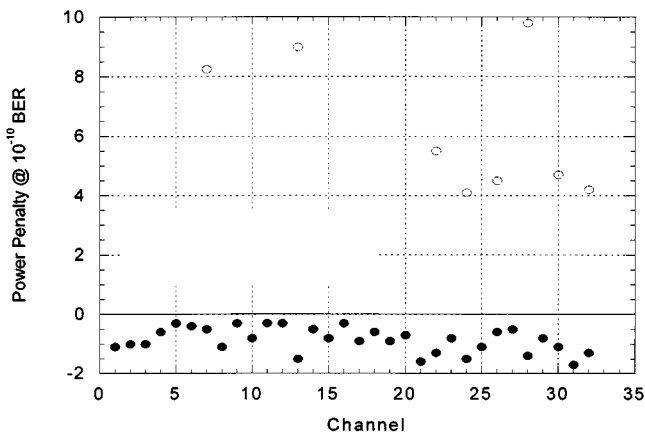


Fig. 17. Comparison of measured power penalties for 32 2.5-Gb/s DMLs after transmission over 300 km of MetroCor (solid circles) and SMF-28 (open circles) fibers.

by the  $Q$ -variations of different channels over the two fibers (Fig. 16). This device dependence is well understood and explained in Sections II-B and II-E.

In order to characterize the different transmission performance of lasers across the channel plan the power and chirp waveforms at the output of the DMLs were measured. In Fig. 18, the results for two channels (ch. 21 and ch. 30) are

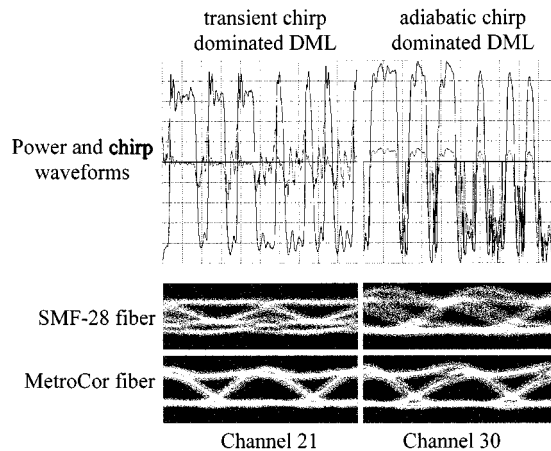


Fig. 18. Power and chirp waveforms for ch. 21 and ch. 30. The received eye patterns at the receiver are also shown for each fiber type.

shown. According to the discussion of Session II, the ch. 21 DML is transient chirp dominated, while ch. 30 is adiabatic chirp dominated. From the received eye patterns for each fiber (Fig. 18), it can be deduced that, for both laser types the transmission performance when using MetroCor fiber is improved. Again, the improvement is greater for the transient chirp dominated laser, showing that the performance is strongly device dependent.

The shape of the received eyes (shown in Fig. 18) can be easily explained through knowledge of the power and chirp waveforms according to the considerations presented in Section II-A. The shapes of the eye diagrams for both transient (ch. 21) and adiabatic (ch. 30) chirp dominated DMLs are in agreement with the results obtained from the transmission performance simulations of two different adiabatic and transient chirp dominated DMLs in Section II-A.

#### H. Operation in the 1310-nm Window

Performance of a negative dispersion fiber in the 1310-nm window may be of interest in some metro applications. Testing

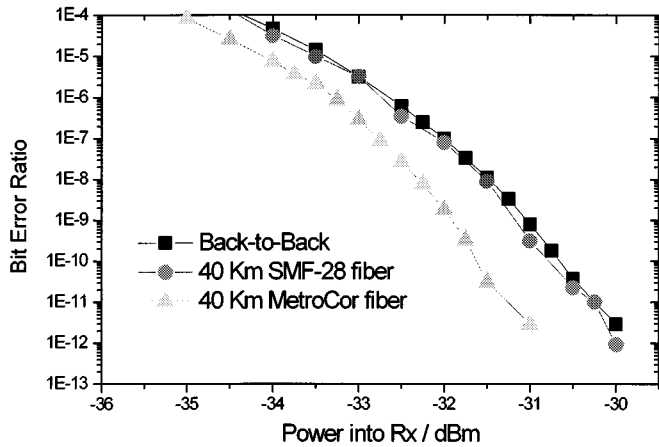


Fig. 19. BER measurements of a 2.5-Gb/s DML at 1310-nm wavelength region before and after transmission over 40 km of SMF-28 (circles) and MetroCor (triangles) fibers. The back-to-back performance is also shown (squares).

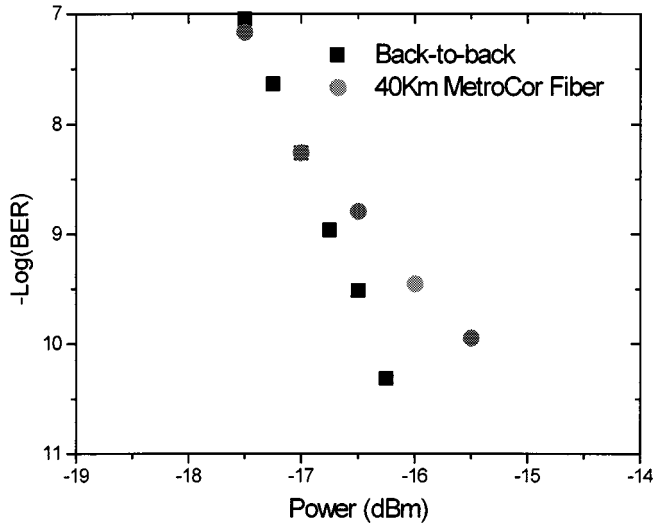


Fig. 20. BER measurements of a 10-Gb/s DML at 1310-nm wavelength region before (squares) and after (circles) transmission over 40 km of MetroCor fiber.

was carried out over up to 60 km of the prototype negative dispersion fiber using five uncooled directly-modulated 1310-nm lasers operating at 2.5 Gb/s. Error-free performance was achieved with all devices up to 60 km, at which point transmission was loss- and not dispersion-limited. For 40-km transmission (ITU-T recommendation), the devices showed negative power penalties ranging between 0.5–1 dB. Fig. 19 shows BER measurements for the signal transmission after 40 km of SMF-28 fiber and MetroCor fibers, together with the back-to-back performance of one of the DMLs. The improved performance of MetroCor fiber in comparison with the SMF-28 fiber is evident. Hence, MetroCor fiber design is compatible over shorter metropolitan distances using 1310-nm DMLs.

For the 1310-nm wavelength region, there are also commercially available 10-Gb/s DMLs. We measured the transmission performance over 40 km of MetroCor fiber using a 10-Gb/s DML and the results are presented in Fig. 20. It is shown that 40-km transmission is possible with a power penalty of less than 1 dB at a BER of  $10^{-10}$ .

### III. STUDY OF THE TRANSMISSION PERFORMANCE OF EA-DFBs OVER METROCOR AND SMF-28 FIBERS AT 10 Gb/s

#### A. Modeling of Electroabsorption Modulated Lasers for System Simulation Purposes

This session addresses the upgradability of networks employing MetroCor fiber without dispersion compensation to 10 Gb/s by using cost-effective electro-absorption modulator integrated DFB laser (EA-DFB's) transmitters. For the simulations, we used the phenomenological electroabsorption modulator model presented in [11]. The model takes into account the dependence of the chirp on the applied bias voltage. Given two sets of experimentally measured data points, the  $\alpha$ -parameter and absorption coefficient versus reverse bias voltage, it computes the complex envelope of the modulated electric field at the output of the device.

#### B. Transmission Simulations Using 10-Gb/s EA-DFB Transmitters

Using the aforementioned EA-DFB model, we performed simulations to compare the transmission performance of 10-Gb/s signals over SMF-28 and MetroCor fibers. All simulations were performed using 10-dB extinction ratio. The sign of the chirp-parameter was set opposite to the sign of the dispersion of the fiber in each case by properly adjusting the reverse bias voltage of the electroabsorption session. The simulations were repeated for different operating wavelengths across the *C*- and *L*-bands and the results for both fiber types are shown in Fig. 21. The eye-closure penalty is plotted versus link length for transmission over SMF-28 and MetroCor fibers. The solid lines represent results obtained when the transmission wavelength is at the outer edges of the *C*- and *L*-bands (1530 and 1622 nm, respectively). The broken line represents the results for a wavelength of 1570 nm. It is shown that for a channel-wavelength of 1622-nm (curve 4) transmission over MetroCor fiber shows a negative penalty for distances up to 600 km, while transmission over SMF-28 fiber (curve 1) shows a penalty of 2 dB at a distance of 80 km. For a wavelength of 1530 nm, transmission over MetroCor fiber (curve 3) reaches the 2-dB limit at a length larger than 200 km, while the performance over SMF-28 fiber is limited to no more than 120 km (curve 2). Since the chirp parameter is optimized for each fiber, in all cases, a small negative power penalty can be achieved at a certain distance (ranging from 40 to 50 km for SMF-28 fiber, and from 100 to 600 km for MetroCor fiber).er outperforms SMF-28 fiber for channels across both *C*- and *L*-bands.

#### C. Transmission Experiments Using 10-Gb/s EA-DFB Transmitters

The transmission performance was measured for a single channel system employing EA-DFBs and MetroCor or SMF-28 fiber. The chirp characteristics of EA modulated lasers can be varied by changing the bias and drive voltages on the EA modulator [11], [12]. Decreasing the reverse bias voltage on an EA-DFB makes the chirp  $\alpha$ -parameter more positive. Concurrently, the output power increases as the reverse bias voltage decreases. However, the extinction ratio decreases when biasing for a more positive chirp  $\alpha$ -parameter. The interaction

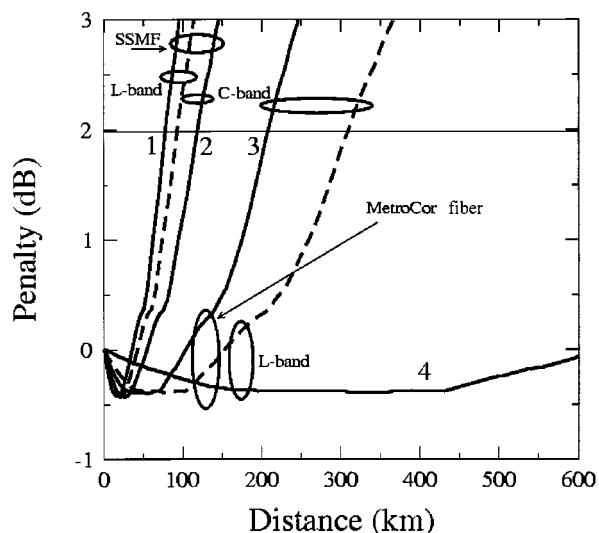


Fig. 21. Calculated eye closure penalty versus distance of a 10-Gb/s electroabsorption-modulated laser for transmission over SMF-28 and MetroCor fibers. The solid lines represent results obtained when the transmission wavelength is at the outer edges of the C- (1530 nm—curves 2,3) and L- (1622 nm—curves 1,4) bands. The broken line represents the results for a wavelength of 1570 nm.

of the chromatic dispersion with the chirp will produce pulse compression if the dispersion is negative (MetroCor fiber) and the chirp  $\alpha$ -parameter is positive or if the dispersion is positive (SMF-28 fiber) and the chirp  $\alpha$ -parameter is negative. Based on the above consideration, the best drive conditions (for a  $Q$ -factor greater than 8.5 dB) were found for maximum reach of the EA-DFBs through each fiber type. Thus, two sets of drive conditions, one for MetroCor fiber and one for SMF-28 fiber were used. At 1555 nm and 10 Gb/s, the reach of the system with a system  $Q$ -factor higher than 8.5 dB using MetroCor fiber was found to be more than twice that of the system employing SMF-28 fiber for all EA-DFBs we tested. The system reach was 225 km using MetroCor fiber and only 90 km when using SMF-28 fiber. At this point, we should note that the performance enhancement was achieved for driving conditions of the EA-DFBs that resulted in higher power levels at the output of the device.

These results, clearly show that MetroCor fiber Fig. 22 shows the measured eye patterns before and after transmission over MetroCor fiber and over SMF-28 fiber. The eye patterns at the transmitter side are different because of the different driving conditions that were used to achieve the maximum reach in each case. For the case of MetroCor fiber, the specific driving conditions resulted in a transmitted optical signal with dynamic extinction ratio of 7.3 dB. In the case of SMF-28 fiber, the dynamic extinction ratio was 10.3 dB.

Fig. 23 shows BER measurement versus the received power measured using a preamplified receiver. The length of the PRBS was  $2^{31}-1$ . It is evident, that in the case of SMF-28 fiber, low error rates are achieved with higher power penalties at the maximum link length than the penalties over the maximum link length of MetroCor fiber. In fact, transmission of signals over a length of MetroCor fiber of up to 200 km is achieved with negative power penalties. The maximum negative penalty was about 4.5 dB (at a BER of  $10^{-12}$ ) for a distance of 125 km. This

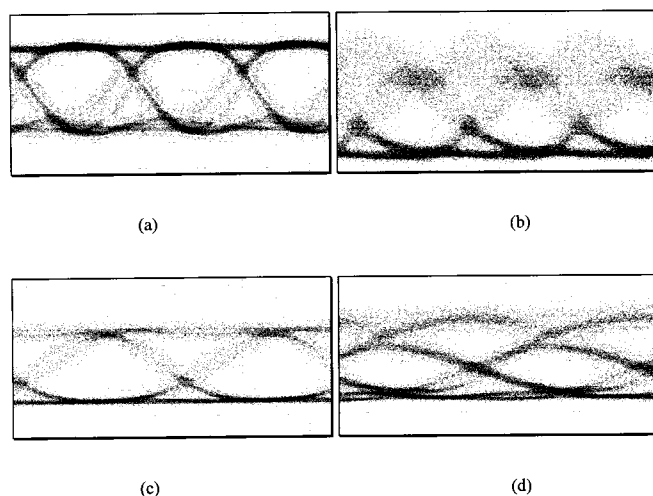


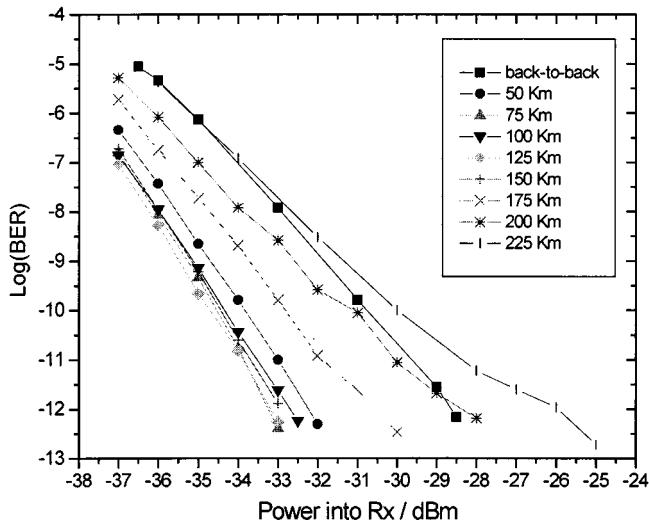
Fig. 22. Measured 10-Gb/s eye patterns after (a) 0 km and (b) 225 km of MetroCor fiber, and after (c) 0 km and (d) 90 km of SMF-28 fiber.

negative power penalty will provide a power margin that can be used to relax the specifications on other optical devices in a Metro network. In the case of SMF-28 fiber, even at a distance of 25 km, there is a power penalty larger than 2 dB at a BER of  $10^{-11}$ .

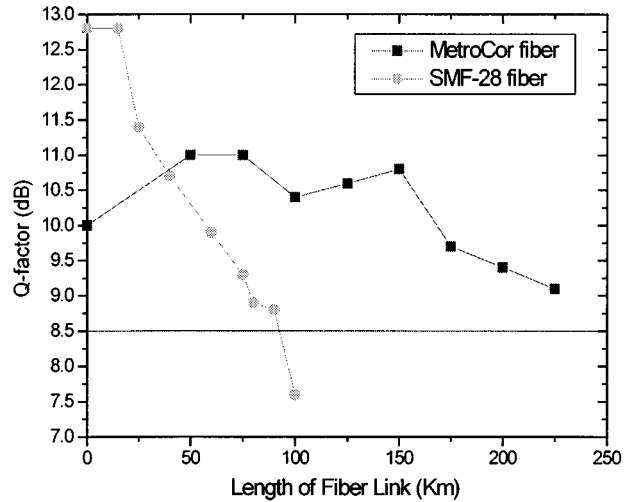
The system using SMF-28 fiber had a higher extinction ratio at the beginning of the link than the system using MetroCor fiber. That resulted in higher back-to-back  $Q$ -factor values and lower receiver sensitivity for the system using the SMF-28 fiber (Fig. 24). However, as the link length was increased a significant degradation in the achievable  $Q$ -factor was observed. The  $Q$ -factor was dropped below the acceptable value of  $Q = 8.5$  dB for a link length of 90 km, while the receiver sensitivity for a BER of  $10^{-9}$  increased about 7 dB to a value of  $-28$  dBm. The results for the MetroCor fiber show that the  $Q$ -factor can be improved by almost 1 dB relative to the back-to-back case, while the receiver sensitivity is decreased by up to 3.5 dB. These results indicate significant performance advantages when using MetroCor fiber in 10-Gb/s applications involving distances of up to 225 km.

#### IV. STUDY OF THE TRANSMISSION PERFORMANCE OF EXTERNALLY MODULATED-MZ OVER METROCOR AND SMF-28 FIBERS AT 10 Gb/s

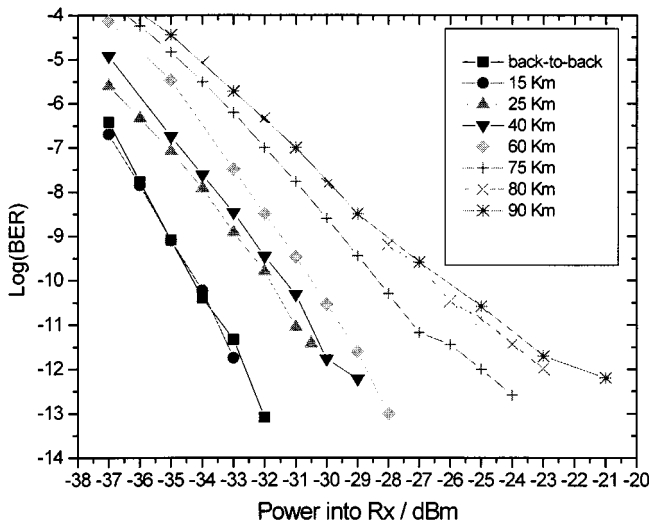
In the future, it is expected that carriers may wish to upgrade their metropolitan networks to 10-Gb/s bit rates, and use more densely spaced channels across the C- and L-wavelength bands. The need for elimination of dispersion compensation will still be a requirement. The transmission distances in metro area networks are much shorter than those in long-haul networks. Consequently, lower optical power levels can be used and the impact of optical nonlinearities is not expected to be very significant (dispersion is still the limiting impairment). This section presents the results of a modeling study that was performed to verify that nonlinearities are not the main limitation for metropolitan area network applications at 10 Gb/s and to predict the maximum uncompensated reach of MetroCor fiber on a DWDM system. It will shown that reaches



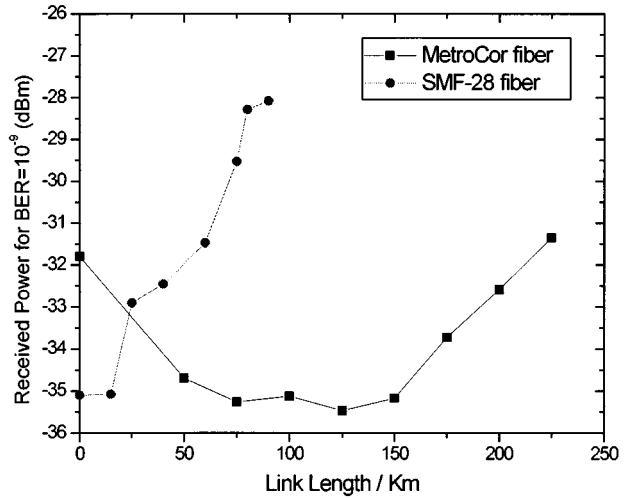
(a)



(a)



(b)



(b)

Fig. 23. (a) Receiver sensitivity in the case of (a) MetroCor and (b) SMF-28 fibers.

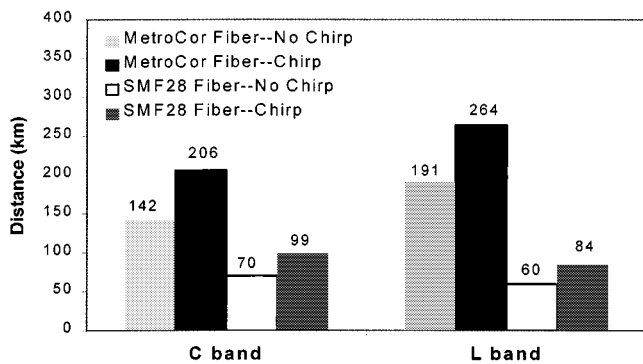
Fig. 24. (a)  $Q$ -factor and (b) receiver sensitivity for a BER of  $10^{-9}$  versus link length for a system incorporating a 10-Gb/s electroabsorption modulated laser and MetroCor (squares) or SMF-28 (circles) fibers.

in excess of 200 km are predicted for both  $C$ - and  $L$ -bands over MetroCor fiber. The maximum reach for MetroCor is compared to the maximum reach of SMF-28 fiber. Both 100- and 200-GHz channel spacings were studied.

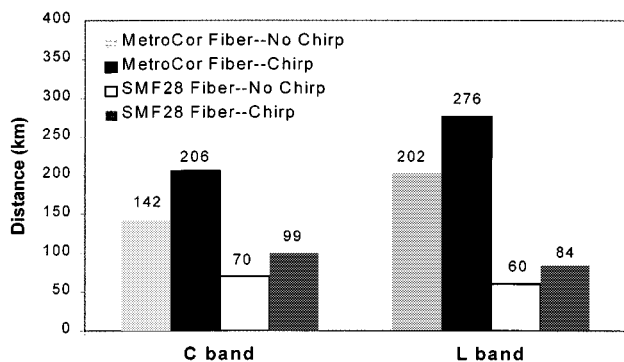
The modeling study was based on a metro area network architecture similar to that illustrated in Fig. 1. The architecture is comprised of a regional transport ring (RTR) and several access rings, each having spans of equal distances. The span lengths were varied in the simulations, with the ratio of RTR span length to access span length for all cases being constant. Access rings are connected to the RTR ring with optical cross connects (OXC), which include an optical switch, multiplexers/demultiplexers, and optical amplifiers with a noise

figure of 7 dB. It is assumed that the switch has 6-dB loss, and the MUX/DMUX pair has 3-dB loss if the signal continues on the RTR ring and 5-dB loss if the signal is connected to an access ring. Amplifier gains were adjusted within the model depending on the length of the spans in order to compensate for the span losses and were considered to have flat gain across all channels. The WADMs between the spans of the access ring are modeled as having 3-dB insertion loss.

Simulations were performed to compute the maximum reach of the system with both fiber types. The maximum reach is defined as the maximum distance that can be achieved for a system with all channels having a total  $Q$ -value greater than 9.5 dB, and



(a)



(b)

Fig. 25. Calculated maximum reach distances of (a) a 40-channel WDM system with 100-GHz channel spacing, and a (b) 20-channel WDM, with 200-GHz channel spacing. Both fibers (MetroCor and SMF-28) are compared across the *C*- and *L*-bands for the cases of no- or optimum-modulator chirp.

an eye closure penalty due to distortion less than 3 dB. Fiber dispersion, fiber loss, modulator chirp, and nonlinearities were the causes of the waveform distortion. The simulations were performed for the two EDFA bands, the conventional *C*-band with channel wavelengths from 1530 to 1565 nm (frequencies from 191.5 to 195.9 THz) and the long wavelength *L*-band, with channel wavelengths from 1570 to 1610 nm (frequencies from 186.2 to 191.0 THz). Two channel plans were studied, (a) a 40-channel WDM system with 100-GHz channel spacing, and (b) a 20-channel WDM with 200-GHz channel spacing. In both channel plans, the wavelengths were set according to the ITU-T grid. An external modulator (lithium niobate MZ type) was used to modulate the optical signals at 10 Gb/s. The study was conducted for two chirp parameters of the modulator for each fiber type (0 and  $\pm 0.7$ ). The sign of the chirp parameter was set opposite to the sign of the dispersion of the fiber in each case (optimum chirp). An input power of 2-dBm per channel was chosen for the simulations. The extinction ratio was 13 dB.

Fig. 25 shows bar charts of the maximum uncompensated reach values for the two fibers, for the two-channel plans (100- and 200-GHz spacing), for both wavelength bands and for the cases of no- or optimum-modulator chirp. Adding modulator chirp significantly increases maximum reach for all fibers in both bands, with the benefit ranging from 24 km for SMF-28 fiber to 74 km for MetroCor fiber, both in the *L*-band. MetroCor

fiber outperformed SMF-28 fiber in both *C*- and *L*-bands with a reach of 206 km in the *C*-band, and 264 km in the *L*-band in the case of 100-GHz spacing [see Fig. 25(a)]. In the case of 200-GHz channel spacing [see Fig. 25(b)], the maximum reach in the *C*-band is unaffected, while it is increased to 276 km in the *L*-band. For both chirp cases and for both channel spacings, the reach of SMF-28 fiber was less than half the reach of MetroCor fiber with the difference being larger in the *L*-band. The very small change in the maximum transmission distance achieved with MetroCor fiber when the channel spacing is reduced from 200- to 100-GHz spacing indicates that the relative small effective area of MetroCor fiber (about  $46 \mu\text{m}^2$  at 1550 nm) in comparison with SMF-28 fiber ( $80 \mu\text{m}^2$  at 1550 nm) is not a concern for Metropolitan area networks.

*Q*-factor profiles across the wavelength bands for all different scenarios were also calculated. The overall results are shown in Fig. 26. Included in each graph are the single channel *Q*-factor profiles and *Q*-factor profile of the fully loaded WDM system. Degradation in single-channel *Q* is caused by waveform distortion due to fiber dispersion, fiber loss, modulator chirp, and self-phase modulation (SPM). In the multichannel case, cross-phase modulation (XPM) and four-wave mixing (FWM) nonlinearities cause additional distortion. *Q*-factor profiles for MetroCor and SMF-28 fibers, with 100- and 200-GHz spacings and with or without modulator chirp are shown in Fig. 26. In the case of MetroCor fiber, the maximum reach distance is limited by the reduced *Q*-factor values. Cross-channel nonlinearities (XPM and FWM) contribute to limiting the reach in the WDM system. At 100 GHz, their effects are more pronounced in comparison to 200-GHz channel spacing. In the case of SMF-28 fiber, the eye-closure penalty due to dispersion is by far the largest hindrance to maximum reach distance for SMF-28 fiber in both the *C*- and *L*-bands. The *Q*-factor values shown in the figure are large, but the eye-closure penalty is 3 dB. Cross channel nonlinearities degrade the *Q*-factor values by a small amount, especially in the case of 100-GHz spacing. The slope of the *Q*-factor profiles is different between the cases of SMF-28 and MetroCor fibers. The sign of the slope is the opposite, because the zero dispersion wavelength in the case of the SMF-28 fiber is at the “blue” side of the wavelength bands under investigation, while in the case of MetroCor fiber is at the “red” side of the wavelength bands.

## V. CONCLUSION

DWDM technologies make effective use of the available fiber bandwidth and offer an added dimension to all-optical networks. Recently, these technologies have been introduced to metropolitan area networks. The requirement that these networks should be cost effective has added complexity to the network engineering. The use of low-cost optical transmitters raises the dispersion-induced limitations to the main impairment that limits the size of metro networks. Dispersion compensation techniques could be adopted as in the case of long-haul networks, but the additional cost and the design complexity prohibit such a solution. An optical fiber especially designed for Metro area applications that will take advantage of the characteristics of low cost transmitters and eliminate

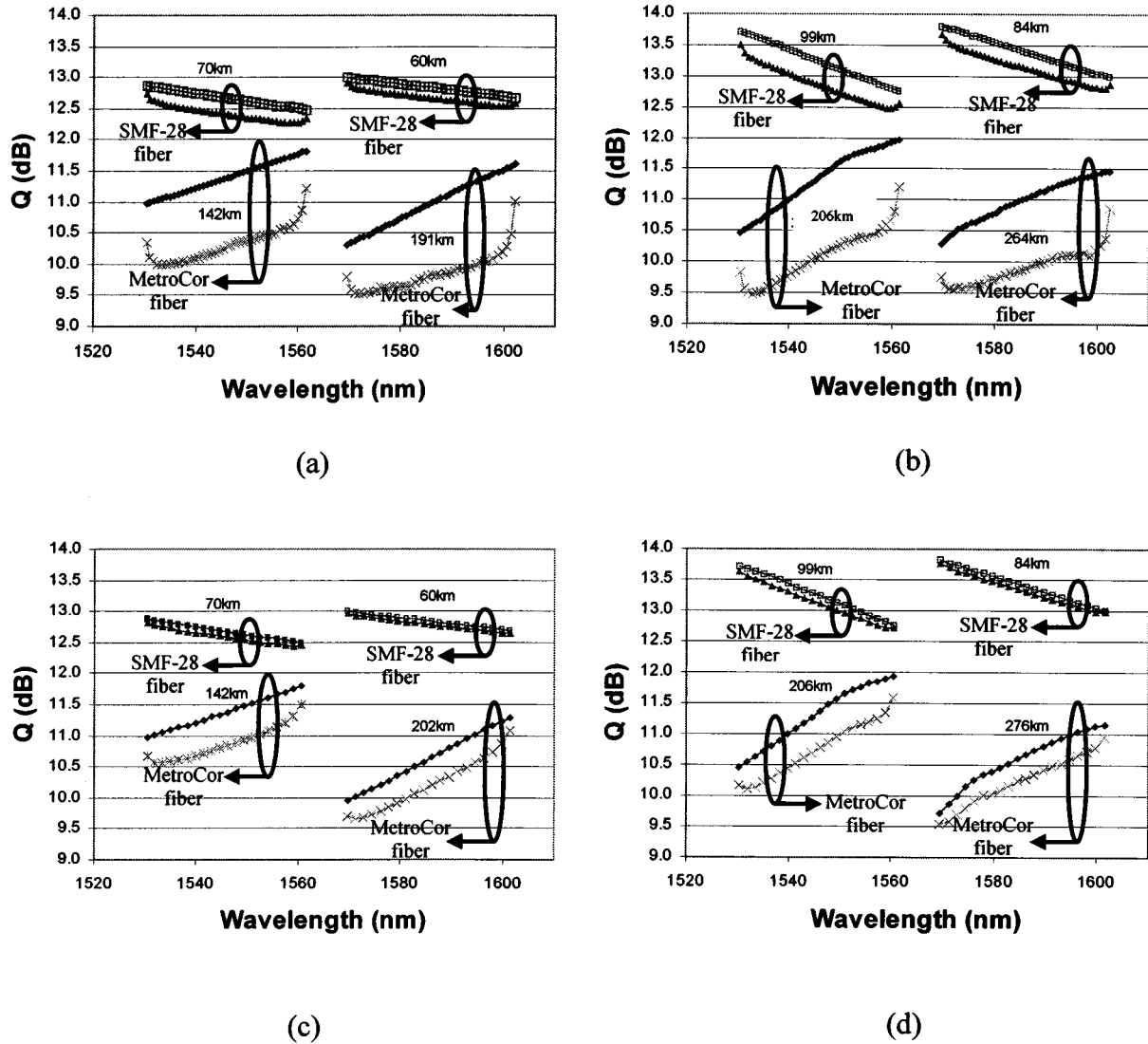


Fig. 26. Calculated  $Q$ -factor profiles across the  $C$ - and  $L$ -bands for (a) 100-GHz channel spacing with no modulator chirp, (b) 100-GHz channel spacing with modulator chirp, (c) 200-GHz channel spacing with no modulator chirp, and (d) 200-GHz channel spacing, with modulator chirp. Squares correspond to single-channel transmission over SFM-28 fiber, triangles correspond to WDM transmission over SFM-28 fiber, diamonds correspond to single channel transmission over MetroCor fiber, and crosses correspond to WDM transmission over MetroCor fiber.

the need for dispersion compensation is highly desirable, and will enable the introduction of DWDM technologies in the metro environment. This work provides a detailed study on the transmission performance of such a novel nonzero dispersion shifted fiber with negative dispersion (MetroCor fiber). The performance of MetroCor fiber was studied using different types of optical transmitters (DMLs, EA-DFBs, MZs). The studies were performed for both 1310- and 1550-nm wavelength windows at 2.5 and 10 Gb/s.

The improved performance of MetroCor fiber relative to a fiber with conventional dispersion characteristics (positive dispersion) is extensively discussed for the case of directly modulated lasers having different chirp characteristics. Through a detailed understanding of the transmission characteristics of transient or adiabatic chirp dominated lasers over fibers with different dispersion characteristics, we show that the performance of MetroCor fiber will always be superior in comparison with that of SMF-28 fiber. It has been shown that

DMLs with transient chirp dominated response give excellent performance for 300 km of MetroCor fiber, where as such DMLs are limited to about 100 km of SMF-28 fiber. DMLs with purely adiabatic chirp dominated response have almost the same dispersion/length product performance for MetroCor and SMF-28 fiber. However, due to the lower absolute value of dispersion, MetroCor fiber will achieve longer transmission distances than SMF-28 fiber. For practical transmitters, where both transient and adiabatic chirp exist, the performance of negative dispersion fibers (MetroCor fiber) in comparison with positive dispersion fibers, will always be superior. In addition, we show that at 10 Gb/s, where the transient chirp increases, the improvement in the transmission performance over MetroCor fiber relative to that over SMF-28 fiber will be more pronounced than that at 2.5 Gb/s. All the theoretical results have been validated through experiments. Using a 32-channel DWDM test bed, it was shown that MetroCor fiber expands the system capabilities up to 300 km in the  $C$ -band.

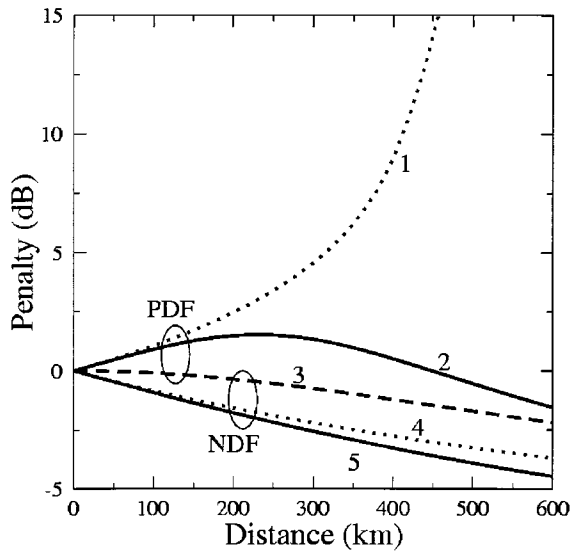


Fig. 27. Calculated power penalty versus transmission distance. Positive dispersion fiber and transient chirp only (curve 1), negative dispersion fiber and transient chirp only (curve 4), both fiber types and adiabatic chirp only (curve 3), positive dispersion fiber and both chirps (curve 2) and negative dispersion fiber and both chirps (curve 5).

Experimental and theoretical results for the case of transmission of 10-Gb/s EA modulated signals over SMF-28 fiber and MetroCor fiber show that improved performance (in terms of maximum reach) is obtained using a negative dispersion fiber. This experimentally observed improvement in performance was achieved when driving the EA-DFBs at voltage levels that resulted in high-power output from the device.

In the case of 10-Gb/s external modulated signals using MZ modulators, computer simulations predict that the maximum reach that can be accomplished with MetroCor fiber in the *C*-band without dispersion compensation is 206 km. In the *L*-band the maximum distance predicted with MetroCor fiber is 264 km for the case of 100-GHz channel spacing, and 276 km for 200-GHz spacing. SMF-28 fiber performed significantly worse than MetroCor fiber. Adding modulator chirp significantly increased the maximum reach for both fibers. Increasing channel spacing resulted in very little or no increase in maximum reach.

In conclusion, we have shown that a NZDSF with negative dispersion (MetroCor fiber) is engineered to enhance optical systems resulting in reduced system costs and complexity, since the need of dispersion compensation is eliminated. MetroCor fiber takes advantage of the characteristics of inexpensive lasers and is expected to enable transparency in metro area optical networks.

#### APPENDIX A

##### SMALL-SIGNAL-BASED MODEL OF DMLS

This appendix presents a rigorous small-signal analysis of the interaction between laser chirp and chromatic dispersion. The target of this small-signal model is to analyze the impact of transient and adiabatic chirp on the performance of fiber types having different dispersion parameter signs. It is shown that the intersymbol interference (ISI) can be attributed to the phase dif-

ference between intensity and frequency modulations in the case of transient chirp dominated lasers.

The instantaneous frequency change (chirp— $\Delta\omega(t)$ ) is given by the following expression:

$$\Delta\omega(t) \cong \frac{\alpha}{2} \left[ \frac{d \ln[P(t)]}{dt} + \kappa P(t) \right] \quad (\text{A.1})$$

where

- $P(t)$  instantaneous optical power;
- $\alpha$  linewidth enhancement factor;
- $\kappa$  adiabatic chirp coefficient.

Taking the Laplace transform of (A.1), it can be shown that the small-signal FM response of a DML is given by the following expression:

$$H_{\text{FM}}(\omega_m) = \frac{\Delta\omega(\omega_m)}{P(\omega_m)} = \frac{\alpha}{2P_0} \sqrt{(kP_0)^2 + \omega_m^2} e^{i \tan^{-1}(\frac{\omega_m}{kP_0})} \quad (\text{A.1})$$

where  $\omega_m$  is the angular modulation frequency and  $P_0$  the average optical power.

For the purpose of this study, a periodic small-signal sinusoidal modulation of both intensity and phase is assumed. Therefore, the power of the optical signal at the output of the DFB semiconductor laser could be expressed as

$$P(t) = P_0(1 + 2m \cos \omega_m t) \quad (\text{A.3})$$

where  $m$  is the AM modulation index.

The output complex envelope of the electric field could be expressed as

$$E(t) \cong \sqrt{2P_0}(1 + m \cos \omega_m t) e^{i\beta \sin(\omega_m t + \phi) + i\omega_d t}. \quad (\text{A.4})$$

In (A.4)  $\beta$  is the frequency modulation (FM) index

$$\beta = \frac{m\alpha}{\omega_m} \sqrt{(kP_0)^2 + \omega_m^2} \quad (\text{A.5})$$

$\phi$  is the phase difference between AM and FM

$$\phi = \tan^{-1} \frac{\omega_m}{kP_0} \quad (\text{A.6})$$

and  $\omega_d$  is a frequency offset

$$\omega_d = \frac{\alpha k P_0}{2} \quad (\text{A.7})$$

The fiber transfer function is given by [27]:

$$H(f) = e^{-i\theta(\frac{f}{f_m})^2} \quad (\text{A.8})$$

where

$$\theta = -\frac{\pi}{c} \lambda^2 D L f_m^2 \quad (\text{A.9})$$

is the phase change due to dispersion,  $\lambda$  is the carrier wavelength,  $D$  is the dispersion parameter at  $(f + f_d)$ ,  $f_m$  is the modulation frequency,  $L$  is the transmission distance and  $c$  is the speed of light in vacuum.

The small-signal model has now been formulated. As an example we will present the simulation results for the following parameter set:  $m = 0.1$ ,  $\beta_{\text{transient-chirp}} +$

$\beta_{\text{adiabatic-chirp}} = 0.5$  (separate chirp types) or  $\beta_{\text{total}} = \sqrt{\beta_{\text{transient-chirp}}^2 + \beta_{\text{adiabatic-chirp}}^2} = 0.707$  (combined chirp types),  $\lambda = 1.55$  mm,  $|D| = 17$  ps/nm/km and  $f_m = 1$  GHz (corresponding to  $R_b = 2$  Gb/s). The simulation results are presented in Fig. 27. It can be seen that the power penalty increases dramatically for large transmission distances, if we transmit a waveform produced by a DML that has only transient chirp over positive dispersion fiber (curve 1). If the same signal is transmitted over a negative dispersion fiber a negative power penalty is obtained (curve 4). For both fiber types and for a DML that has only adiabatic chirp we obtained the same performance (curve 3). If a signal produced by a DML with both transient and adiabatic chirp is transmitted over a positive dispersion fiber we observe a penalty smaller than that in the case of transmission of signal with transient chirp only (curve 2). If the same signal is transmitted over negative dispersion fiber a further more negative power penalty will also be achieved (curve 5). The results show that the transient chirp is deleterious for positive dispersion fibers and beneficial for negative dispersion fibers. No performance improvement is observed if a negative dispersion fibers is used instead of a positive dispersion fiber with the same absolute value of dispersion in the exclusive presence of adiabatic chirp.

It is worth noting that the above small-signal analysis associates the phase difference between amplitude (AM) and frequency (FM) modulations, which is an intrinsic characteristic of all lasers with the dispersion characteristics of the fiber without eliminating either the transient or the adiabatic chirp terms. It is shown that when the AM phase lags compared to FM, the pulses are compressed in a negative dispersion fiber. However, it should be noted that this analytical study is strictly valid for a small-signal sinusoidal waveform. The distortion-induced penalty in the case of large-signal NRZ pulses must be studied using the rate equations-based model.

## REFERENCES

- [1] A. A. M. Saleh and J. M. Simmons, "Architectural principles of optical regional and metropolitan access networks," *J. Lightwave Technol.*, vol. 17, pp. 2431–2448, Dec. 1999.
- [2] N. Antoniadis, A. Boskovic, J. K. Rhee, J. Downie, D. Pastel, I. Tomkos, I. Roudas, N. Madamopoulos, and M. Yadlowsky, "Engineering the performance of DWDM metro networks," presented at the NFOEC'00, Denver, CO, Aug. 2000.
- [3] C. A. Brackett *et al.*, "A scalable multiwavelength multihop optical network: A proposal for research on all-optical networks," *J. Lightwave Technol.*, vol. 11, pp. 736–753, May/June 1993.
- [4] R. E. Wagner *et al.*, "MONET: Multiwavelength optical networking," *J. Lightwave Technol.*, vol. 14, pp. 1349–1355, June 1996.
- [5] S. B. Alexander *et al.*, "A precompetitive consortium on wide-band all-optical networks," *J. Lightwave Technol.*, vol. 17, pp. 2431–2448, Dec. 1999.
- [6] G. Agrawal and N. Dutta, *Long Wavelength Semiconductor Lasers*: Van Nostrand Reinhold, 1986.
- [7] G. P. Agrawal, *Fiber Optic Communication Systems*. New York: Wiley, 1992.
- [8] P. J. Corvini and T. L. Koch, "Computer simulation of high bit rate optical fiber transmission using single frequency lasers," *J. Lightwave Technol.*, vol. LT-5, pp. 1591–1595, Nov. 1987.
- [9] J. C. Cartledge and G. S. Burley, "The effect of laser chirping on lightwave system performance," *J. Lightwave Technol.*, vol. 7, pp. 568–573, Mar. 1989.
- [10] C.-C. Wang, I. Roudas, I. Tomkos, M. Sharma, and R. S. Vodhanel, "Negative dispersion fibers for uncompensated metropolitan networks," presented at the ECOC'00, Munich, Germany, Sept. 2000.

- [11] J. C. Cartledge and B. Christensen, "Optimum operating points for electroabsorption modulators in 10 Gb/s transmission systems using nondispersion shifted fiber," *J. Lightwave Technol.*, vol. 16, pp. 349–357, Mar. 1998.
- [12] G. Ishikawa, H. Ooi, K. Morito, K. Kamite, Y. Kotaki, and H. Nishimoto, "10 Gb/s optical transmission systems using modulator integrated DFB lasers with chirp optimizing," in *Proc. ECOC'96*, 1996, p. 245. paper WeP.09.
- [13] K. Hintkan and T. Stephens, "Modeling high-speed optical transmission systems," *IEEE J. Select. Areas Commun.*, vol. 11, pp. 380–392, Apr. 1993.
- [14] T. L. Koch and R. A. Linke, "Effect of nonlinear gain reduction on semiconductor laser wavelength chirping," *Appl. Phys. Lett.*, vol. 48, pp. 613–615, Mar. 1986.
- [15] A. V. T. Cartaxo, "Small signal analysis for nonlinear and dispersive optical fibers and its application to design of dispersion supported transmission systems with optical dispersion compensation," in *IEE Proc. Part J—Optoelectronics*, vol. 146, 1999, pp. 213–222.
- [16] "Comparison of different DFB laser models within the European COST 240 collaboration," in *IEE Proc.-Optoelectron.*, vol. 141, Apr. 1994, pp. 82–88. COST 240 group.
- [17] L. M. Zhang and J. E. Carrol, "Large signal dynamic model of the DFB laser," *IEEE J. Quantum Electron.*, vol. 28, pp. 604–611, 1992.
- [18] S. Hansmann, H. Burkhard, H. Walter, and H. Hillmer, "A tractable large signal dynamic model—Application to strongly coupled distributed feedback lasers," *J. Lightwave Technol.*, vol. 12, pp. 952–956, 1994.
- [19] A. J. Lowery, "Transmission-line modeling of semiconductor lasers: The transmission-line laser model," *Int. J. Numer. Model.*, vol. 2, pp. 249–265, 1990.
- [20] L. Bjerkan, A. Royset, L. Hafskjaer, and D. Myhre, "Measurements of laser parameters for simulation of high speed fiber-optic systems," *J. Lightwave Technol.*, vol. 14, pp. 839–850, May 1996.
- [21] J. C. Cartledge and R. C. Srinivasan, "Extraction of DFB laser rate equation parameters for system simulation purposes," *J. Lightwave Technol.*, vol. 15, pp. 852–860, May 1997.
- [22] K. Czotscher, S. Weisser, A. Leven, and J. Rosenzweig, "Intensity modulation and chirp of 1.55  $\mu\text{m}$  multiple quantum well laser diodes: Modeling and experimental verification," *IEEE J. Select. Topics Quantum Electron.*, vol. 5, pp. 606–612, May/June 1999.
- [23]
- [24] R. A. Linke, "Modulation induced transient chirping in single frequency lasers," *IEEE J. Quantum Electron.*, vol. QE-21, pp. 593–597, June 1985.
- [25] B. W. Hakki, "Evaluation of transmission characteristics of chirped DFB lasers in dispersive optical fiber," *J. Lightwave Technol.*, vol. 10, pp. 964–970, July 1992.
- [26] S. Mohrdiek, H. Burkland, F. Steinhagen, H. Hillmer, R. Losch, W. Schlapp, and R. Gobel, "10 Gb/s standard fiber transmission using directly modulated 1.55 quantum-well DFB lasers," *IEEE Photon. Technol. Lett.*, vol. 7, pp. 1357–1359, Nov. 1995.
- [27] O.-K. Kwon and J.-I. Shim, "The effects of longitudinal gain distributions on the static and the dynamic properties in a  $\lambda/4$  phase-shifted DFB laser," *IEEE J. Quantum Electron.*, vol. 34, pp. 225–232, Feb. 1998.
- [28] A. F. Elrefaie, R. E. Wagner, D. Atlas, and D. G. Daut, "Chromatic dispersion limitations in coherent lightwave transmission systems," *J. Lightwave Technol.*, vol. LT-6, pp. 704–709, May 1988.
- [29] *Synch. Optical Network (SONET): Physical Layer Specifications*, ANSI T1.105.06.
- [30] *Optical Interfaces for Equipments and Systems Relating to the Synchronous Digital Hierarchy*, ITU Recommendation G. 957, July 1995.

**Ioannis Tomkos** received the B.Sc. degree in physics, the M.Sc. degree in telecommunications engineering from the University of Patras, Greece, and the Ph.D. degree in optical telecommunications from the University of Athens, Athens, Greece, in 1994, 1996, and 2000, respectively.

He was with the Optical Communications Laboratory, University of Athens, Athens, Greece, as a Research Fellow, where he participated in several national and European research projects (e.g., ACTS, COST). He researched novel wavelength conversion technologies based on nonlinear effects in semiconductor optical amplifiers and fibers. He is currently with Corning, Inc., Somerset, NJ, where he is a Senior Research Scientist. His current research focuses in transport issues related with optical networks. He is currently leading efforts related with transport performance and technology trends in metropolitan/regional area optical networks. He is author or co-author of about 50 papers.

Dr. Tomkos has received awards for his research accomplishments from The International Society for Optical Engineers (SPIE), Bellingham, WA, and IEEE.

**Dipak Chowdhury** received the B.Sc. degree in electrical engineering from Bangladesh University of Engineering and Technology, Dhaka, Bangladesh, in 1986, and the M.S. and Ph.D. degrees in electrical engineering from Clarkson University, Potsdam, NY, in 1989 and 1991, respectively.

From 1991 to 1993, he had a joint appointment as a research associate at Yale University, New Haven, CT, in the Applied physics department and at New Mexico State University, Las Cruces, NM, in the Electrical Engineering Department. For his graduate and post-graduate work he performed numerical modeling of and experimentation on optical scattering from nonlinear microcavities. He joined Corning's research and development facility, Somerset, NJ, in 1993. He focused his research effort in various aspects of optical communication systems. Currently, he is managing modeling and simulation research in fiber-optic communication systems and optical devices. His research interests include linear and nonlinear devices, impairments in fiber-optic systems and networks, e.g., nonlinearities, cross-talk, chromatic dispersion, and polarization-mode dispersion, and efficient algorithms for simulating fiber-optic systems.

**Jan Conradi** received the B.Sc. degree in engineering physics from Queen's University, Kingston, ON Canada, the M.Sc. degree in solid state electronic engineering from the University of Birmingham, U.K., the Ph.D. degree in solid state physics from Simon Fraser University, Burnaby, BC, Canada, in 1962, 1964, and 1968, respectively.

He was with the RCA Labs, Montreal, Canada, where he developed Silicon avalanche photodetectors for early fiber-optic systems at 820 nm. He then moved to Bell Northern Research, Ottawa, Canada, (the Research and Development arm of Nortel Networks), where he managed various groups responsible for optical fiber development, fiber to the home systems, as well as two FTTH field trials, and the company's exploratory research for progressively higher bit rate fiber systems. He also had research projects on Mobile Radio, and Scanners & Printers. He was an industrial research chair professor at the research consortium TR Labs and the University of Alberta. In December 1997, he joined Corning Inc., Somerset, NJ, as the first manager of external research, then as core technology director, fiber communications, where he was responsible for leading the evolution of Corning Inc. research programs for the company's next generations of optical fiber. Currently, he is director of Strategy for Corning Optical Communications.

Dr. Conradi is a fellow of the Optical Society of America (OSA). He has served on numerous conference committees, including chairman of OFC, has been associate editor of *Optics Letters*, the JOURNAL OF LIGHTWAVE TECHNOLOGY, and IEEE PHOTONICS TECHNOLOGY LETTERS.

**D. Culverhouse**, was with the University of Southampton as a Senior Research Fellow, where his research interests included nonlinear optics and switching and fiber-based components. From 1997 to 1999, he joined Corning Inc. as a research scientist, where he worked within amplifier development. Currently, he is the Business Development Manager for Metropolitan Networks, where he acts as the technical lead when addressing optimized fiber designs and cost effective solutions for metropolitan-based architectures.

**K. Ennser**, photograph and biography not available at the time of publication.

**Cynthia Giroux** received the B.Sc. and M.E. degrees in metallurgy and materials science from Carnegie-Mellon University, Pittsburgh, PA.

She is with Corning Incorporated, Somerset, NJ, where she manufactures optical fiber and components, as well as development of glass and coating processes for transmission fiber products. Most recently, she was leader of the cross-functional technical team, which investigated and developed negative dispersion fiber (MetroCor fiber) for the metropolitan market.

**Bradley S. Hallock** received the B.S. degree in physics from State University of Cortland New York, in 1988.

He is currently with Corning Incorporated, Somerset, NJ, where he conducts photonic measurement and fiber-optic systems research.

**Timothy D. Kennedy**, received the associates of science degree from the University of Phoenix, Phoenix, AZ, in 1991.

From 1973 to 1995, he served in the United States Army, where he was the Communications and Electronics Installation and Technical Evaluation Chief. In 1995, he was with AT&T. In 1996, he joined Lucent Technologies as a Senior Technical Associate in the Advanced Technology Division. In 1997, he joined Corning Incorporated at the Photonics research and Test Center, Somerset, NJ, as an optical fiber systems technologist. Recently, he has worked on dense wavelength-division-multiplexing systems experiments to support the commercial introduction of a negative dispersion fiber (MetroCor fiber) for the metropolitan market.

**Ann Kruse** received the B.S.E.E. and M.S.E.E. degree specializing in optics and electromagnetics from the University of Missouri at Rolla, in 1992 and 1997, respectively, and the B.S.Ed. and M.S.Ed. degrees with majors in elementary education and mathematics, and teaching of reading from Concordia Teacher's College, Seward, NE and Northwest Missouri State University of Maryville, respectively.

While at UMR, she taught a laboratory class and a communications systems class. She then joined the network architecture team at WorldCom, Tulsa, Oklahoma, where she developed network availability models for both terrestrial and undersea networks, participated in standards activities, and participated in vendor product evaluation. In 1999, she joined Corning, Inc., Photonic Research & Test Center in Somerset, NJ, where she is a Senior Scientist currently working on modeling.

**S. Kumar**, photograph and biography not available at the time of publication.

**N. Lascar**, photograph and biography not available at the time of publication.



**Ioannis Roudas** was born in 1966 in Athens, Greece. He received the diploma in Physics and the Certificate in electronics and radio-engineering from the University of Athens, Greece, and the M.S. and Ph.D. degrees from Ecole Nationale Supérieure des Télécommunications (ENST) Paris, Paris, France, in 1988, 1990, 1991, and 1995, respectively. His Ph.D. thesis concerned modeling and optimal design of coherent optical communication systems.

From 1995 to 1998, he was with the Optical Networking Research Department at Bell Communications Research, Red Bank, NJ, where he was involved in the multiwavelength optical networking (MONET) project. His research mainly focused on the development of an efficient computer representation of the MONET optical transport layer. He was also an Adjunct Professor in Electrical Engineering at Columbia University during the fall semesters 1997 and 1998. Since 1999, he is a Senior Research Scientist in the Photonic Research and Test Center of Corning Inc., Somerset, NJ. His current research concerns modeling of transmission effects in high data rate optical communications systems and networks.

Dr. Roudas serves as a reviewer for the IEEE Optical Society of America (OSA) JOURNAL OF LIGHTWAVE TECHNOLOGY and the IEEE PHOTONICS TECHNOLOGY LETTERS.

**Manish Sharma** received the M.Eng. degree in electrical and electronic engineering from the University College London, London, U.K., and the Ph.D. degree from Sophia University, Tokyo, Japan, in 1990 and 1998, respectively.

From 1990 to 1998, he was engaged in the research and development of optical communication systems and networks at Toshiba Corporation, Tokyo, Japan. In 1998, he joined Corning Incorporated as a Senior Research Scientist at the Photonic Research and Test Center. His research interests include dense wavelength-division-multiplexing (DWDM) optical networking systems and components.

**R. S. Vodhanel** received the B.S., M.S., and Ph.D. degrees in physics from the University of California, Irvine, CA, in 1974, and from the University of Illinois, Urbana-Champaign, IL, in 1976 and 1980, respectively.

From 1980 to 1984, he conducted research in the single-mode fiber transmission systems at AT&T Laboratories. In 1984, he joined Bellcore, where his research concerned coherent optical communications systems, dense wavelength-division-multiplexing (DWDM) transmission in metropolitan, and long-haul networks as part of the Multiwavelength Optical Networking (MONET) Consortium. In 1997, he joined Tellium Inc. as a founding member, where he developed optical transmission products for metropolitan and long-haul markets. Since 1999, he has been a Research Manager with Corning Inc., Photonics Research and Test Center, Somerset, NJ. His current research interests include DWDM transmission on novel optical fibers.

**C.-C. Wang**, photograph and biography not available at the time of publication.